

**PERFORMANCE EVALUATION OF GREEN  
SURFACTANT FOR EOR PROCESSES**

BY

**Ahmed Saeed Al Ghambi**

A Thesis Presented to the  
DEANSHIP OF GRADUATE STUDIES

**KING FAHD UNIVERSITY OF PETROLEUM & MINERALS**

DHAHRAN, SAUDI ARABIA

In Partial Fulfillment of the  
Requirements for the Degree of

**MASTER OF SCIENCE**

In

**PETROLEUM ENGINEERING**

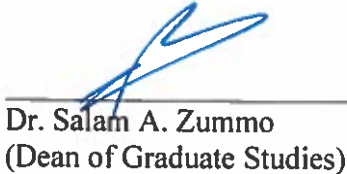
**April 2019**

KING FAHD UNIVERSITY OF PETROLEUM & MINERALS  
DHAHRAN- 31261, SAUDI ARABIA  
DEANSHIP OF GRADUATE STUDIES

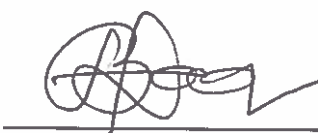
This thesis, written by Ahmed Saeed Al Ghamdi under the direction of his thesis advisor and approved by his thesis committee, has been presented and accepted by the Dean of Graduate Studies, in partial fulfillment of the requirement for the degree of Master of Science in Petroleum Engineering.



Dr. Dhafer Al-Shehri  
(Department Chairman)

  
Date ١٥/١٠

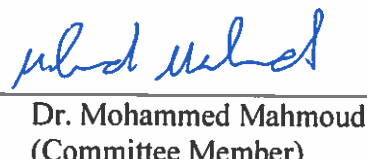
Dr. Salam A. Zummo  
(Dean of Graduate Studies)



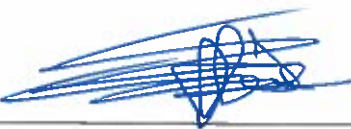
Dr. Bashirul Haq  
(Advisor)



Dr. Dhafer Al-Shehri  
(Co-Advisor)



Dr. Mohammed Mahmoud  
(Committee Member)



Dr. Abdulaziz Al Majed  
(Committee Member)



Dr. Rahul Gajbhiye  
(Committee Member)

*I would like to dedicate this thesis to my parents and my wife, who have stood behind me, helped me, and supported me throughout this work and throughout my studies. I couldn't have done it without their invaluable support.*

© Ahmed Saeed Al-Ghamdi

2019

## ACKNOWLEDGEMENT

Firstly, I would like to acknowledge my advisor, Dr. Bashirul Haq, and my co-advisor, Dr. Dhafer Al-Shehri. Their guidance and assistance during my thesis work were invaluable contributions to this study.

Also, my highest appreciation must be extended to Saudi Aramco, who have sponsored and supported me during this degree program. It was their support that made this study possible.

I would also like to thank my committee members, Dr. Abdulaziz Al Majed, Dr. Mohamed Mahmoud, and Dr. Rahul Gajbhiye; their helpful input and suggestions throughout the process were instrumental to the improvement and finalization of this work.

I would like to thank Expec Advanced Research Center at Saudi Aramco, Dr. Abdulkarim Al Sofi for availing his lab. I would like to thank Abdullah Al Boqmi for running the spinning drop tensiometer experiments.

I must also give my thanks to BASF, for their kind contribution of Glucopon® 600 CSUP, which was used in the formulation of green surfactant mixtures in this study.

## TABLE OF CONTENTS

ACKNOWLEDGEMENT .....	v
TABLE OF CONTENTS .....	vi
LIST OF FIGURES .....	x
LIST OF TABLES .....	xii
LIST OF ABBREVIATIONS .....	xiv
ABSTRACT .....	xvii
ملخص الرسالة .....	xix
CHAPTER ONE - INTRODUCTION .....	1
1.1.    Introduction.....	1
1.2.    Overview of Enhanced Oil Recovery Methods .....	2
1.2.1. Thermal EOR .....	2
1.2.2. Gas EOR.....	3
1.2.3. Chemical EOR .....	3
1.3.    Selection of Surfactants .....	14
1.4.    Objectives and Scope of this Study .....	16
1.5.    Overview of the Experimental and Simulation Work .....	17
1.5.1. Phase Behavior.....	18
1.5.2. Fluid Properties Tests.....	18
1.5.3. Core-Flooding Tests.....	19

1.5.4. Simulation of Core-Flooding Experiment.....	19
1.6. Thesis Structure and Organization.....	19
CHAPTER TWO – COMPREHENSIVE LITERATURE SURVEY.....	21
2.1. Rhamnolipids .....	21
2.2. Alkyl Polyglycosides .....	25
2.4. Lecithin .....	28
2.5. Summary and Knowledge Gap.....	29
CHAPTER THREE - METHODOLOGY.....	31
3.1. Materials .....	31
3.2. Phase Behavior Study .....	32
3.2.1. Introduction .....	32
3.2.2. Background .....	35
3.2.3. Experiments.....	37
3.3. Fluid Properties Tests .....	39
3.3.1. Sample Preparation .....	39
3.3.2. Density Measurements .....	40
3.3.3. Viscosity Measurements .....	43
3.3.4. Interfacial Tension Measurements .....	46
3.4. Core-Flooding Tests .....	51
3.4.1. Introduction.....	51

3.4.2. Apparatus .....	52
3.4.3. Procedure.....	55
3.5. Simulation of Core-Flooding Experiment .....	60
3.5.1 Introduction .....	60
3.5.2 Background .....	61
3.5.3 Input Format.....	65
3.5.4 Model Description.....	66
CHAPTER FOUR - RESULTS AND DISCUSSION .....	69
4.1. Phase Behavior Study .....	69
4.1.1. Rhamnolipid and 1-Butanol (Set RB) .....	70
4.1.2. Rhamnolipid, APG, and 1-Butanol (Set RAB) .....	72
4.1.3. Rhamnolipid and Lecithin (Set LR) .....	74
4.2. Fluid Properties Tests .....	76
4.2.1. Viscosity Measurement Results .....	76
4.2.2. Density Measurement Results.....	76
4.2.3. Interfacial Tension Measurement.....	77
4.3. Core-Flooding Tests .....	84
4.3.1. Core Properties.....	84
4.3.2. Core Experiment #1 .....	85
4.3.3. Core Experiment #2 .....	88

4.3.4. Core Experiment #3 .....	91
4.3.5 Comparison of the Three Formulations .....	94
4.4. Simulation of Core-Flooding Experiment .....	96
4.4.1 Formulation 1: Rhamnolipid and 1-Butanol .....	96
4.4.2 Formulation 2: Rhamnolipid, APG, and 1-Butanol .....	99
4.4.3 Formulation 3: Rhamnolipid and Lecithin .....	102
4.5 Conclusions.....	105
4.6 Recommendations.....	107
APPENDIX A .....	108
A.1. Rhamnolipid Literature Survey Summary .....	108
A.2. APG Literature Survey Summary .....	109
APPENDIX B.....	111
B.1. Simulation Input Data for Formulation RB .....	111
B.2. Simulation Input Data for Formulation RAB.....	111
B.3. Simulation Input Data for Formulation RL.....	112
REFERENCES .....	113
VITAE .....	122

## LIST OF FIGURES

Figure 1 – Microemulsion phase types. Taken from the work of Sheng (2011) .....	34
Figure 2 - DMA 4500 Anton Paar Densitometer .....	42
Figure 3 - Tamson TV4000 thermostatic visibility bath .....	45
Figure 4 - M6500 Spinning Drop Tensiometer.....	49
Figure 5 - FDES-645Z core-flooding apparatus.....	53
Figure 6 - FDES-645Z core-flooding apparatus, inside-oven view .....	54
Figure 7 – Modeled three-dimensional Cartesian rectangular grid .....	68
Figure 8 - Results of the phase behavior study (set RB) .....	71
Figure 9 - Results of the phase behavior study (set RAB) .....	73
Figure 10 - Results of the phase behavior study (set LRF) .....	75
Figure 11 - Plot of the IFT against the rhamnolipid concentration, set A.....	79
Figure 12 - Plot of the IFT against the rhamnolipid concentration, set B .....	81
Figure 13 - Plot of the IFT against the rhamnolipid concentration, set C .....	83
Figure 14 - Oil recovery vs. cumulative injection (Core #1) .....	87
Figure 15 - Oil recovery vs. cumulative injection (Core #2) .....	90
Figure 16 - Oil recovery vs. cumulative injection (Core #3) .....	93
Figure 17 – Comparison of the oil recovery for the developed formulations .....	95
Figure 18 - Total oil recovery observed during core flooding and simulation for the first formulation .....	98

Figure 19 - Total oil recovery observed during core flooding and simulation for the second formulation .....	101
Figure 20 - Total oil recovery observed during core flooding and simulation for the third formulation .....	104

## LIST OF TABLES

Table 1 - HLB ranges and their uses. Reproduced from Griffin's 1949 work .....	7
Table 2 - List of materials .....	31
Table 3 - List of optimized formulations and their salinity scan variations .....	38
Table 4 - Surfactant and co-solvent concentration data for set A .....	40
Table 5 - Surfactant, cosurfactant, and co-solvent data for set B .....	40
Table 6 - Surfactant and cosurfactant concentration data for set C.....	40
Table 7 - Cell and simulation model dimensions .....	66
Table 8 - Viscosity measurements of the crude oil and brine .....	76
Table 9 - Density of the crude oil, brine, and surfactant mixture samples.....	77
Table 10 - IFT values of the formulated surfactant samples, set A.....	78
Table 11 - IFT values of the formulated surfactant samples, set B.....	80
Table 12 - IFT values of the formulated surfactant samples, set C.....	82
Table 13 - Properties of the three Berea sandstone cores used in the core-floods.....	84
Table 14 - Measured and observed data for the core flooding experiment (Core #1).....	86
Table 15 - Measured and observed data for the core flooding experiment (Core #2).....	89
Table 16 - Measured and observed data for the core flooding experiment (Core #3).....	92
Table 17 - Summary of the EOR results for the three formulations. ....	94
Table 18 - Literature Survey Summary, Rhamnolipid .....	109
Table 19 - Literature Survey Summary, APG .....	110
Table 20 - Relative permeability and saturation data for formulation #1 (RB) .....	111
Table 21 - Fluid property data for formulation #1 (RB) .....	111

Table 22 - Relative permeability and saturation data for formulation #2 (RAB) .....	111
Table 23 - Fluid property data for formulation #2 (RAB).....	111
Table 24 - Relative permeability and saturation data for formulation #3 (RL).....	112
Table 25 - Fluid property data for formulation #3 (RL).....	112

## LIST OF ABBREVIATIONS

ACN – Alkane carbon number: The number of carbons in a simple alkane oil.

APG – Alkyl polyglycoside: A synthetic green surfactant.

API – Also called API gravity, stands for American Petroleum Institute gravity - A measure of crude oil density compared to water.

BPR – Back pressure

Cc – Characteristic curvature:

CH<sub>2</sub> – Methylene group

CMC – Critical micelle concentration: A concentration of surfactant in solution that leads to the surfactant molecules congregating into micelles.

DOT – Dispersant-to-oil: A ratio between oil and the fluid it's dispersed in.

EACN – Equivalent alkane carbon number – A dimensionless number used to predict the hydrophobicity of oil.

EC50 – Effective concentration: A toxicity measurement used to measure surfactant toxicity in daphnia and algae.

EOR – Enhanced oil recovery: Methods of tertiary oil recovery that extend beyond traditional water and immiscible gas flooding.

GEOR – Green enhanced oil recovery: Techniques for EOR that are environmentally friendly.

**HLB** – Hydrophile-Lipophile Balance: A concept that attempts to classify surfactants and predict their behavior.

**HLD** – Hydrophilic-Lipophilic Difference/Deviation: A concept developed to predict surfactant behavior in the company of certain oils.

**IFT** – Interfacial tension: A value measuring the tension between two fluids at their interface.

**LC50** – Lethal concentration: A toxicity measurement used to measure surfactant toxicity in fish.

**OOIP** – Original oil in place: Refers to the original amount of oil in a reservoir before any kind of recovery attempts have been made.

**O/W** – Used to describe an oil-in-water emulsion.

**P<sub>o</sub>** – Cumulative oil production.

**PPM** – Parts per million: A ratio of 1 : 1,000,000.

**PV** – Pore volume: Usually refers to the pore volume of a Berea sandstone core.

**PV<sub>o</sub>** – The amount of pore space containing oil.

**PV<sub>w</sub>** – The amount of pore space containing water.

**SMEDS** – Self-microemulsifying delivery system.

**S<sub>o</sub>** – Oil saturation.

**S<sub>or</sub>** – Residual oil saturation.

**S<sub>w</sub>** – Water saturation.

$S_{wr}$  – Residual water saturation.

TOR – Tertiary oil recovery

W/O – Used to describe a water-in-oil emulsion.

## ABSTRACT

Full Name: Ahmed Saeed Al-Ghamdi

Thesis Title: Performance Evaluation of Green Surfactant For EOR Processes

Major Field: Petroleum Engineering

Date of Degree: April 2019

Surfactant flooding is a promising form of chemical enhanced oil recovery (EOR).

It has been proven capable of recovering significant amounts of oil after secondary recovery methods, such as water-flooding, have been exhausted. However, synthetic surfactants are environmentally concerning, causing more and more people to look for less toxic methods to recover the residual oil. This has sparked an interest in green surfactants, which are safer for the environment. These surfactants are now being studied for their possible uses in green chemical EOR processes. The biosurfactant rhamnolipid, the green nonionic surfactant alkyl polyglycoside (APG), and the green surfactant lecithin are examples of green surfactants, but they have not been thoroughly studied for their potential in chemical EOR. In this study, blends of rhamnolipid, lecithin, and APG are considered as possible formulations in chemical EOR. Phase behavior studies, fluid property measurements, core-flooding experiments, and simulation studies are performed to investigate the efficacy of these green surfactant formulations in sandstone reservoirs. The three developed formulations performed well in the phase behavior study, with all three forming stable middle phase microemulsions. In the core flooding tests, the first

formulation was able to achieve almost 23% tertiary recovery and 62% of the OOIP; the second didn't perform as well as expected, with the incremental oil recovery due to surfactant flooding reaching only around 10%, and a total recovery of 55%; the third formulation performed the best of the three, with a tertiary recovery of 24% and nearly 70% total recovery. Simulations of the core flooding experiments were done with a black oil simulator, and matched quite well with the experimental values. Tertiary oil recoveries from the simulation were 26%, 12%, and 24% for each respective formulation, and total oil recoveries of 63%, 55%, and 67% were obtained. Both the rhamnolipid/butanol and the rhamnolipid/lecithin formulations performed strongly in the experiments, demonstrating excellent potential for application in EOR processes.

## ملخص الرسالة

الاسم الكامل: أحمد سعيد العامدي

عنوان الرسالة: قياس اداء عناصر السطح الفعالة الخضراء في عمليات استخلاص النفط المعزز

التخصص: هندسة البترول

تاريخ الدرجة العلمية: ابريل 2019

يُعتبر الغمر بعناصر السطح الفعالة تقنية ذات مستقبل واعد في مجال عمليات الاستخلاص الكيميائي المعزز للنفط حيث انها اثبتت قدرتها على استخلاص كميات كبيرة من النفط المتبقى بعد انتهاء عمليات استخلاص النفط الثانوية مثل الغمر بالماء، عناصر السطح الفعالة الصناعية لها تأثير سلبي على البيئة مما دفع كثيرا من الباحثين للبحث عن طرق اقل سمية لاستخلاص النفط المتبقى. وقد اثار هذا الاهتمام في عناصر السطح الفعالة الخضراء ، حيث انها اكثر آماناً للبيئة. وتم الان دراسة امكانية استخدام عناصر السطح الفعالة الخضراء في عمليات استخلاص النفط المعزز الخضراء. يعد العنصر السطحي الفعال الاحيائى rhamnolipid والعنصر السطحي الفعال الغير ايوني alkyl polyglycoside (APG) والعنصر السطحي الفعال lecithin أمثلة على العناصر السطحية الفعالة الخضراء التي لم تتم دراسة امكانية استخدامها في عمليات استخلاص النفط المعزز الخضراء بشكل كافي. خلال هذه الدراسة، تم التتحقق من امكانية استخدام عدة تركيبات مكونة من خليط من lecithin و APG و rhamnolipid في مجال عمليات الاستخلاص الكيميائي المعزز للنفط. تم اجراء اختبارات سلوك المواقع وقياس خواص السوائل و تجارب الغمر الفيضي ودراسات المحاكاة لمعرفة مدى فاعلية تركيبات العناصر السطحية الفعالة الخضراء في استخلاص النفط المتبقى من مكامن الصخور الرملية. كان أداء التركيبات المطورة في هذه الدراسة جيداً في اختبارات سلوك المواقع حيث انها شكلت طوراً متوسطاً ثابتاً. استخلصت التركيبة الاولى ما يقارب 23% خلال المرحلة الثالثة من الاستخلاص و 62% من كمية النفط الاصلية، أما اداء التركيبة الثانية فلم يكن جيداً كما كان متوقعاً ، حيث بلغت نسبة الاستخلاص للنفط بحسب الغمر بعناصر السطح الفعالة ما يقرب من 10% فقط ، ونسبة الاستخلاص الكلي 55% من كمية النفط الاصلية. كان أداء التركيبة الثالثة هو الأفضل بين الثلاثة حيث انها استخلصت 24% خلال مرحلة الاستخلاص الثالثة و استخلصت 70% من كمية النفط الاصلية. تم اجراء محاكاة لتجارب الغمر الفيضي باستخدام برنامج محاكاة للنفط الاسود وتوافقت النتائج من برنامج المحاكاة مع القيم المختبرية خلال تجارب الغمر الفيضي. كانت نسبة الاستخلاص خلال

المرحلة الثالثة باستخدام برنامج المحاكاة 26% و 12% و 24% للتركيبيات الثلاثة و كانت نسبة الاستخلاص الكلية 63% و 55% و 67% للتركيبيات الثلاثة. كان اداء التركيبة المكونة من rhamnolipid و butanol و اداء التركيبة المكونة من lecithin و rhamnolipid جيداً مما يدل على ان لهم امكانيات ممتازة في مجال عمليات الاستخلاص الكيميائي المعزز للنفط.

## CHAPTER ONE - INTRODUCTION

### 1.1. Introduction

For many years, engineers have been developing and researching methods to increase the recovery of oil from reservoirs. Standard recovery methods often fall far short of the full amount of oil held in any given reservoir, due to high capillary forces trapping the oil in place and pressure loss as the level of oil in the reservoir drops. Primary recovery, where the oil is recovered using the natural energy contained in the reservoir—energy from the solution-gas drive, natural waterdrive, fluid and rock expansion, gas-cap drive, and gravity drainage—recovers only about 35% of the original oil in place (OOIP). Other methods, such as waterflooding or immiscible gas injection for pressure maintenance or displacement of the oil towards the wellhead are used as secondary methods, which can further the recovery up to around 50%, on average (Green & Wilhite, 1997). Other sources suggest that the primary and secondary recovery methods combined may recover as little as one-third of the OOIP in a given reservoir (Roehl & Choquette, 1985).

These statistics suggest that as much as 65% of residual oil remains in the reservoir, unrecoverable by traditional methods of recovery due to uneconomical cost of continued secondary recovery methods or due to the trapping mechanisms holding the oil in place. This is where enhanced oil recovery (EOR) comes in.

## 1.2. Overview of Enhanced Oil Recovery Methods

EOR is the practice of injecting materials (usually fluids or gases) into the reservoir for any purpose other than simple displacement of the oil. It's usually aimed at lowering the interfacial tension (IFT) between the oil and the surrounding fluid, allowing the oil to flow and reach the production well (Green & Wilhite, 1997). Various methods of releasing the trapped oil so that it can be recovered have been researched and implemented as tertiary oil recovery methods. Most of these methods of EOR fall under three classifications: Thermal, chemical, or gas.

### 1.2.1. Thermal EOR

Thermal methods of EOR generally involve one of three things: Hot water injection, steam injection, or in-situ combustion for heat generation. These methods are primarily used in reservoirs with very heavy, viscous crude oils, because heat can decrease the viscosity of the oil and the injection of hot water or steam can help displace it towards the production well (Green & Wilhite, 1997).

### 1.2.2. Gas EOR

The injection of miscible gases that will interact with the oil and the reservoir surroundings is considered to be an EOR method, separate from the immiscible gas injection used in secondary recovery methods. Carbon dioxide, hydrocarbon gases, nitrogen, and flue gases are often used in this type of EOR.

### 1.2.3. Chemical EOR

Chemical enhanced oil recovery involves the injection of various chemical fluids into the reservoir, such as polymers and surfactants. These fluids interact with the oil and the surrounding environment through their phase behavior properties, lowering the IFT between the oil and the displacing fluid and allowing the trapped oil to move out of the pores of surrounding rock formations (Green & Wilhite, 1997).

Studies show that chemical EOR is a very promising technique for residual oil recovery, especially in the case of surfactant flooding. A report compiled in 1984 by the National Petroleum Council suggested that with technological advances, chemical enhanced oil recovery techniques may recover up to 40% of the total residual oil recovered through EOR processes. (National Petroleum Council, 1984)

### 1.2.3.1. Surfactants

“Surfactants” is a shortened term referring to the phrase “surface-active agents”. These agents are amphiphilic compounds, generally consisting of a polarized hydrophilic head molecule and a nonpolar lipophilic hydrocarbon tail. The ionic head portion may be cationic, anionic, non-ionic, or even zwitterionic/ampholytic, meaning that they have a dual charge. At low concentrations, surfactants tend to congregate at the surface of a fluid, lowering the surface tension. As the surfactant concentration approaches the critical micelle concentration (CMC), the molecules begin to group together into micelles, and the lowering effect on the IFT becomes negligible with any further increases (Green & Wilhite, 1997).

Because of the separate hydrophilic and hydrophobic moieties, surfactants are soluble in both water and lipids. In an oil/water system, surfactants gather at the interface of the two fluids, emulsifying them and lowering the interfacial tension between them. This makes them very useful for oil recovery purposes (Sheng, 2011).

The number of surfactants that are currently available range into the thousands, which poses a challenge for anyone who is formulating a surfactant or surfactant mix for a given application. In formulating surfactants for enhanced oil recovery, a surfactant must have excellent interfacial tension reduction qualities. This quality can be measured physically in the laboratory using a spinning drop tensiometer or any other device that performs a similar function. However, this measurement is usually time consuming, and measuring IFT reduction for each surfactant or surfactant blend being screened becomes increasingly difficult. Fortunately, it was established by several researchers that the IFT

reduction abilities of a surfactant are closely related to its ability to solubilize oil and water and form a so-called “middle phase” microemulsion phase (Healy, Reed, & Stenmark, 1976). By capitalizing on this observation, the effectiveness of the IFT reduction property can be deduced by conducting a series of relatively inexpensive and fast phase behavior tests.

#### 1.2.3.1.1. Surfactant Characterization

In order to facilitate the understanding and predict the behavior of surfactants, several classification schemes have been proposed over the years. One of the most common one is the classification by the ionic charge of the hydrophilic portion of the surfactant. Using this classification, surfactants can be grouped into four categories:

- Anionic surfactants: the hydrophilic head of the surfactant is ionized and carries a negative charge when dissolved in an aqueous solution. This category is commonly used in EOR as it has good IFT reduction properties and a low adsorption rate on sandstone, as the rock surface is negatively charged.
- Non-ionic surfactant: the hydrophilic head of the surfactant is neutral and does not ionize when dissolved in an aqueous phase. This class of surfactant is less effective in lowering the IFT than an anionic surfactant, but it is often combined with anionic surfactants to improve their tolerance to salinity and water hardness.
- Cationic surfactants: the hydrophilic head of the surfactant is ionized and carries a positive charge when dissolved in an aqueous solution. This category is rarely

used in EOR since it suffers from high losses due to adsorption on the surface of reservoir rocks.

- Zwitterionic surfactants: the hydrophilic head of the surfactant is ionized and carries two types of charges, positive and negative, when it is dissolved in an aqueous solution. This class of surfactant is usually too expensive to be economically utilized in EOR.

Another popular scheme is based on the balance of the molecular weight of the different moieties in the surfactant. This scheme is detailed in the following section.

1.2.3.1.1.1. The Hydrophile-Lipophile Balance. The Hydrophile-Lipophile Balance concept, otherwise known as HLB, was developed by Griffin in 1949 as a way of classifying surfactants and predicting their behavior in an oil-water-surfactant system. HLB is a number that indicates the balance between the hydrophilic and lipophilic portions of a surfactant molecule, where higher and lower numbers describe how hydrophilic or lipophilic the surfactant is. Griffin believed that the HLB number could predict what the surfactant could be expected to achieve, that is, whether it would create an oil-in-water emulsion (O/W), water-in-oil emulsion (W/O), or other distinct behavior differences. The range of HLB numbers and their expected behavior is illustrated in **Table 1**. He noted that the HLB number could not predict how efficiently the surfactant would perform the expected action (Griffin, 1949).

HLB Range	Use
4-6	W/O emulsifiers
7-9	Wetting agents
8-18	O/W emulsifiers

<b>13-15</b>	Detergents
<b>15-18</b>	Solubilizing

Table 1 - HLB ranges and their uses. Reproduced from Griffin's 1949 work

The HLB numbers of various surfactants were determined by Griffin purely through experimental data, performed over many years and through a multitude of different tests. However, he developed a correlation for determining the optimum HLB via a surfactant blend for the type of oil being used in a given test. This “required HLB” referred to the surfactant HLB value required for a specific type of oil to create a specific type of emulsion, and was stated to be achievable by blending surfactants with different HLB values. This value can be determined using the Griffin correlation:

$$\frac{W_A HLB_A + W_B HLB_B}{W_A W_B} \text{ (optimum ratio)} = HLB \text{ oil}$$

Where:

- $W_A$  = The mass of the first surfactant (A)
- $W_B$  = The mass of the second surfactant (B)
- $HLB_A, HLB_B$  = The assigned HLB values of the two surfactants
- $HLB \text{ oil}$  = The required HLB of the oil to achieve the desired type of emulsion.

In a later paper, published in 1954, a multitude of correlations were developed by Griffin for the calculation of the HLB of different types of non-ionic surfactants. He noted that ionic surfactant HLB data could not be calculated using his correlation, stating that the experimental methods used in previous work would have to be used instead (Griffin, 1954).

In 1957, Davies expanded on the work of Griffin, stating that coalescence kinetics were responsible for the type of emulsion created by a given surfactant. He developed a relation that related the HLB number of a surfactant to its chemical formula using the concept of group numbers. Group numbers were assigned to the different hydrophilic and lipophilic groups that constitute a given surfactant. The developed relation is expressed as:

$$HLB = \sum \text{Hydrophilic Group Numbers} - n \times \text{group number per } CH_2 \text{ group} + 7$$

Where  $n$  is the number of  $CH_2$  groups in the surfactant. Using his relation, he calculated the HLB number for several surfactants and found that his results were in good agreement with the HLB numbers obtained through the experimental work conducted by Griffin (Davies, 1957).

While Griffin showed that surfactants could be classified and their behavior predicted by their HLB numbers, he admitted that even surfactants possessing an identical HLB number could not be expected to behave exactly the same, stating that the overall chemical structure of the surfactant had to be taken into account (Griffin, 1949). However, over time, the literature has shown more and more clearly that the HLB method is unreliable even as a general behavior indicator. Shear rate, temperature, and oil concentration, among other influences, have been shown to affect the behavior of a surfactant to the point that O/W emulsions have been prepared with surfactants with HLB numbers resting anywhere from 2 to 17 on the scale (Shinoda & Arai, 1964; Boyd et al., 1972; Kloet & Schramm, 2002; Rosen & Kunjappu, 2012).

### 1.2.3.2. Green Chemical EOR

Due to environmental concerns, green enhanced oil recovery, or GEOR, has become more popular in recent years, and many scientists and engineers have been developing and studying biochemicals for use in EOR methods. It was discovered that various strains of bacteria living in the reservoirs can produce biosurfactants that have been found to be just as effective, if not even more so, as the lab-developed synthetic chemical surfactants largely in use today (Torres et al., 2011). One of these biosurfactants, rhamnolipid, is the focus of this study. Other green surfactants, like alkyl polyglycoside (APG) and lecithin, will be used as co-surfactants in various formulations. A green alcohol, 1-butanol, will be used as a co-solvent.

#### 1.2.3.2.1. Rhamnolipids

Rhamnolipid is a biosurfactant produced by the bacteria strain *Pseudomonas aeruginosa*. The rhamnolipid biosurfactant is considered to have high potential in EOR processes, as it has excellent emulsification properties and strong IFT-lowering properties. In various other studies, it has been shown to lower the surface tension of water from 72 mN/m to 29 mN/m or less (Torres et al., 2011), and phase behavior studies performed using various crude oils has shown IFT reduced as low as 0.05 dynes/cm (Xiangdong, et al., 2007 and Khaleel, 2017, among others in the literature.).

*P. aeruginosa* is a Gram-negative, rod-shaped bacterium that is considered fairly unique in its ability to adapt to all kinds of environments. It is considered a facultative

anaerobe, which is an organism that is able to thrive in the presence of oxygen via aerobic respiration, but can also survive in the absence of oxygen through fermentation or anaerobic respiration (Williams et. al, 2007).

A drawback to rhamnolipid production is that *P. aeruginosa* is considered a class II opportunistic pathogen, making it somewhat risky to work with the bacteria directly (Marchant & Banat, 2012). While it is also produced by two related bacteria strains that are nonpathogenic, *Pseudomonas chlororaphis* (Gunther IV et. al, 2005) and *Burkholderia thailandensis* (Dubeau et. al, 2009) as well as a strain of *Bacillus SP* (Banat I. M., 1993), these bacteria strains produce a different rhamnolipid mixture than the more well-known *P. aeruginosa* microbes (Marchant & Banat, 2012). Also, these newer discoveries have not yet been studied as much as their better-known relative.

#### 1.2.3.2.2. Alkyl Polyglycoside

Alkyl polyglycoside (APG) is a type of non-ionic surfactant that is synthesized using renewable resources such as coconut oil, palm kernel oil, and rapeseed oil for the hydrophobic fatty “tail”, and starches such as wheat, corn, or potatoes for the hydrophilic “head” portion. Because of this, as well as the fact that it’s readily biodegradable and is nontoxic with no identifiable risk to the environment, it’s considered a green surfactant, although it is a synthetic product rather than a biosurfactant (Hill, von Rybinski, & Stoll, 1997). The most common form of APG synthesis is an acid-catalyzed reaction of glucose with various alcohols, which is known as the Fischer synthesis. It was proposed by Emil

Fischer in 1893, and is considered the most economical APG synthesis process for the production of APG surfactant on a commercial scale (Hill, von Rybinski, & Stoll, 1997).

While their IFT lowering properties aren't usually able to create ultra-low IFT environments on their own (Iglauer et. al, 2009), the advantage of APG surfactants is that they tend to be mostly unaffected by temperature and salinity levels (Hill, von Rybinski, & Stoll, 1997). This makes them ideal as a co-surfactant, because they can be mixed with a more effective primary surfactant to reduce the effects of temperature and salinity on the mixture. It should also be noted that combining APG surfactants with specific types of alcohols as co-solvents can also produce effectively low IFT values for EOR purposes (Iglauer et. al, 2009).

#### 1.2.3.2.3. Lecithin

Lecithin is a zwitterionic, phospholipid-based surfactant that is primarily produced from soybeans, but can also be extracted from other oil-bearing seeds and from certain non-vegetable sources like egg yolks. It is heavily used as an emulsifier in the food industry, but the excellent surface-active properties of lecithin can lend themselves well to other products and industries as well.

To produce soy lecithin, soybeans are crushed to extract their oil, which contains phosphorus. The oil is then processed to remove the phospholipids, which can then be purified and dried to make lecithin powders or granules.

One promising aspect of lecithin is that it can be modified in multiple ways to change the behavior of the surfactant to suit the needs of the formulator. These

modifications are generally performed for the purpose of making this very hydrophobic surfactant more hydrophilic. Taken from the work of van Nieuwenhuyzen (2010), the current options for lecithin modifications are:

- Enzymatic and chemical adaptation of the phospholipid molecules
- Physical fractionation for separating oil from the phospholipids
- Fractionation of phospholipids

Because lecithin can be sourced from renewable and inexpensive resources like soybeans and sunflower seeds, it is a green surfactant with promising potential for economical EOR processes.

#### 1.2.3.3. Environmental Concerns

As was mentioned previously, chemical EOR is considered to be one of the most promising types of enhanced oil recovery. There is a drawback to it, however; the chemicals involved in the processes are often environmentally concerning.

Over the years, the toxicity of traditional synthetic surfactants has become more and more of an issue. As awareness of the environmental aspects of our actions increases, studies and experiments determining the effect of these actions have also become commonplace in an effort to determine what can be changed to lessen detrimental effects to the environment wherever possible. The case of surfactants is no exception.

It has been found that many of the surfactants used today have significant toxicity to the environment, such as sodium dodecyl sulfate (SDS), alkyl sulfates (AS),

alkylpolyoxyethylene sulphates (AES), polyoxyethylene alkyl ethers (AE), polyoxyethylene alkylphenyl ethers (APE), and alkyl benzene sulfonates (ABS) (Abd-Allah, 1995; Barbieri, et al., 1998; Susmi, et al., 2010; Liwarska-Bizukojc, et al., 2005). Disposing of these surfactants is often left to wastewater treatment plants, where aerobic microbial action is expected to break down the surfactant to the point that it will cause no harm in the environment when the treated water is released (Kronberg, et al., 2014). Unfortunately, the surfactants are often not readily biodegradable, which means that a large portion of them end up in lakes, rivers, and streams, where the pollution and the effect of it on aquatic life is rapidly becoming visible (Pittinger, et al., 1993; Stalmans, et al., 1995; Romanelli, et al., 2004; Liwarska-Bizukojc, et al., 2005; Abel, 1974; Abel, 1976; Mallatt, 1985).

Studies performed on fish that had been exposed to surfactant waste even in levels as low as 0.5 ppm showed negative effects (Bardach, et al., 1965). The higher the concentration of the surfactants in the water, the more significant the detrimental effects become, with high concentrations shown to kill large numbers of fish (Lewis, 1991; Romanelli, et al., 2004).

To help determine the level of negative impact that a surfactant poses to the environment, several standard measures were developed; some to measure the biodegradability of the surfactant in the environment, and others to show what level of surfactant would be lethal to fish, algae, and daphnia. As an example of biodegradability parameters, for a surfactant to be *readily biodegradable* it should reach 60% biodegradation within 28 days in laboratory tests. The toxicity parameters are measured using LC<sub>50</sub> and EC<sub>50</sub>, which refer to Lethal Concentration and Effective Concentration,

respectively. LC<sub>50</sub> is used to measure toxicity in fish, while EC<sub>50</sub> is used for daphnia and algae. Toxic levels are defined as levels below 1 mg/L after 96 hours of testing on algae and fish, and 48 hours of testing on daphnia, while levels above 10 mg/L are considered to be environmentally benign (Kronberg, Holmberg, & Lindman, 2014).

It has been found that biosurfactants have lower toxicity levels and higher biodegradability, making them a better choice for chemical EOR processes (Georgiou, et al., 1992; Poremba, et al., 1991; Zajic, et al., 1977). The bacteria strains that produce these biosurfactants can often be incubated with renewable feed stock sources, such as molasses (Patel & Desai, 1997), which also contributes to their “green” title. Also, there is the fact that their critical micelle concentration (CMC) levels are often far lower than those of their synthetic counterparts, meaning that less of them will be used overall and so there will be less pollution as a whole (Desai & Banat, 1997; Rebello et al., 2014).

### 1.3. Selection of Surfactants

The criteria for the surfactants selected in this study were as follows:

- The surfactant must be green.
- The primary surfactant must be an anionic surfactant, due to their superior IFT-lowering properties.
- The co-surfactant should preferably be non-ionic, because they aren't easily affected by high levels of temperature and salinity.
- The co-solvent alcohol must be green.

To be classified as a green surfactant, a surfactant must be proven to be both nontoxic and biodegradable, as well as being synthesized from renewable resources. Some green surfactants are biosurfactants, which means that they are synthesized from living organisms such as bacteria or fungi. Others may be synthetic surfactants that fit the above-mentioned criteria to be labeled as green (Lichtfouse, Schwarzbauer, & Robert, 2013).

To select the surfactants, an intensive survey of the literature was performed, found in Chapter 2 of this study. It was found that rhamnolipid, a very promising anionic biosurfactant, has not been extensively studied for its use in EOR techniques. However, the studies performed on rhamnolipid as a bioremediation agent showed that it had a lot of potential as an EOR surfactant.

APG was selected as one of the co-surfactants because of its high resistance to temperature and salinity, which can help create a more stable surfactant formulation for the harsh environment of the typical oil reservoir.

Lecithin was selected because its hydrophobic nature is useful for the purpose of balancing the hydrophilic nature of the primary surfactant, rhamnolipid, to create stable middle phase microemulsions. Also, while lecithin has not been widely used for EOR techniques in the literature, it has shown promise as a surfactant in multiple other industries as well as in soil and sea water bioremediation (Rocchio, et al., 2017; Fava & Gioia, 2001).

A cosolvent alcohol was chosen because bacterium naturally produce alcohols as a byproduct of their cellular respiration processes, especially in the case of anaerobic

respiration. 1-butanol was chosen specifically as the cosolvent because a previous study indicated that it improved the performance of the surfactant formulations that were tested (Haq, 2012).

#### 1.4. Objectives and Scope of this Study

The primary objective of this study is to evaluate the potential of using green surfactants, such as the biosurfactant, rhamnolipid, which is produced by the bacteria strain *P. aeruginosa*, as well as alkyl polyglycoside (APG) and others, in surfactant flooding as a means of enhanced oil recovery in sandstone reservoirs. The alcohol 1-butanol will be tested for its effectiveness as a co-solvent in various formulations.

The objectives of this study are:

- To determine the ability of the biosurfactant rhamnolipid; the green surfactants APG and lecithin; and the cosolvent 1-butanol to reduce the IFT to effectively low levels for enhanced oil recovery needs in various formulated surfactant blends.
- To find the optimal surfactant-cosurfactant-cosolvent formulation for maximum performance in EOR processes.
- To discover the potential of the most effective surfactant formulations to recover an economically significant amount of residual oil via core-flooding experiments using Berea sandstone cores.
- To optimize our surfactant formulations by simulating the previously performed core-flood experiments using a commercial simulator that has been optimized to take into account chemical EOR techniques.

There are very few studies focused on the application of environmentally-friendly surfactants in enhanced oil recovery processes, and even fewer studies studied the performance of surfactant formulations entirely made up of green products. In this study, I intend to bridge this knowledge gap by focusing entirely on green surfactant formulations and testing them for their potential for chemical flooding in sandstone reservoirs. This objective will be achieved by conducting the following experiments:

- Salinity scans will be performed to determine the optimum salinity and study the phase behavior of the surfactant formulations, and to determine the characteristic curvature ( $C_c$ ) value of each surfactant for the purpose of optimizing each surfactant blend.
- Fluid properties experiments will be used to determine the critical micelle concentration (CMC) and the IFT of the various formulations, to help determine the surfactant formulation that is best able to achieve ultralow IFT levels.
- Core-flooding experiments will be performed to estimate the recovery potential under simulated reservoir conditions.
- A simulation of the core-flooding experiments will be performed to further optimize the developed surfactant formulations.

## 1.5. Overview of the Experimental and Simulation Work

In the methodology section, found in Chapter 3 of this study, the details of the tests and studies that were performed will be extensively described. Below is a brief overview of those tests.

### 1.5.1. Phase Behavior

The study of the phase behavior of surfactant systems is essential for understanding and predicting their efficiency in EOR. The goal of most phase behavior studies is to locate the regions of middle phase microemulsion. Middle phase microemulsions are linked to low interfacial tension values, an important factor in oil recovery. The phase behavior of surfactant systems is complex and dependent on several factors. These factors include the type and concentration of surfactants, type of hydrocarbons, brine salinity, and temperature. This study focuses on developing surfactant formulations that exhibit regions of middle phase microemulsion.

### 1.5.2. Fluid Properties Tests

Viscosity, density and interfacial tension are some of the important fluid properties in EOR processes. For a surfactant or surfactant mixture to be viable for EOR purposes, they must reduce the IFT between the oleic and aqueous phases to an ultra-low value. In this study, the density of the formulated surfactant blends, and the viscosity of the crude oil and brine, are measured. Later, using the values obtained from the density measurements, the IFT of the developed surfactant mixtures will be determined using a spinning drop tensiometer.

### 1.5.3. Core-Flooding Tests

Core-flooding experiments are performed under common reservoir pressure and temperature levels to predict the expected behavior of the surfactant inside of a reservoir. The amount of oil recovered by a given surfactant during a core-flood can give a good indication of the possible recovery under normal reservoir conditions. Three core-flood tests were performed using the surfactant formulations that displayed the lowest IFT values in the previous fluid properties study.

### 1.5.4. Simulation of Core-Flooding Experiment

In this part of the study, a commercial reservoir simulator is used to model the surfactant core-flooding experiment. A three-dimensional Cartesian model having the same volume as the cores is constructed, with rectangular grids being used to simplify the modelling process. The fluid properties for the surfactant formulations along with those of the oil and brine are incorporated into the model. Oil recovery from the waterflooding and surfactant flooding phases is generated by running the simulation model, and the results will then be compared to those obtained during the core flooding experiments.

## 1.6. Thesis Structure and Organization

This thesis consists of four chapters; the first chapter gives a general overview of the work that has been covered in this study, with the second chapter providing a

substantial literature review covering the use of green surfactants rhamnolipid, APG, and lecithin by previous researchers, in addition to identifying gaps in today's literature regarding these surfactants. The third chapter details the materials and methods employed in this study. The fourth and final chapter presents the results obtained from the various experiments, discussion of these results, and the conclusions that we can take from them. Recommendations for future research are also suggested. A summary of the literature review in tabular format can been seen in Appendix A.

## CHAPTER TWO – COMPREHENSIVE LITERATURE SURVEY

### 2.1. Rhamnolipids

Xiangdong, et al. (2007) used genetic engineering to clone the genetic information from a strain of *P. aeruginosa* (Rhamnolipid-producing bacteria) into six different strains of *E. coli* bacteria, engineering the *E. coli* bacteria to produce the rhamnolipid biosurfactant. The produced rhamnolipids were purified, dried, and then dissolved into a final concentration of 250ppm.

Using a spinning drop tensiometer, the IFT analysis of the produced biosurfactant was performed. 250ppm of the biosurfactant and 1.5 $\mu$ L of n-octane were used in the analysis. Compared to a value of 35 dyne/cm between the n-octane and water, the IFT between the prepared Rhamnolipid solution and n-octane was a 0.3 dyne/cm.

In addition, the recovery potential of the produced rhamnolipid was evaluated via a sand-pack flooding experiment. They reported a recovery of approximately 40% of the residual oil by the non-engineered *P. aeruginosa* rhamnolipid product at a concentration

of 250ppm, while the products of three of the engineered *E. coli* strains recovered 25-45% of the residual oil at a concentration of 200ppm.

In the work of Amani (2015a), rhamnolipid was produced in a bioreactor by a strain of *P. aeruginosa* (HATH) using sunflower oil as substrate. The produced biosurfactant was found to have a CMC of 120 mg/L, and was tested for stability at various temperatures, salinity values, and pH levels. It was found to remain effective from pH levels between 4 and 10, temperatures as high as 100° C, and salinity concentrations up to 25g/L.

The produced rhamnolipid was shown to reduce the surface tension of water from 72 dyne/cm to 25 dyne/cm, and a minimum value of 2 dyne/cm was obtained for the IFT between a 34° API crude oil and the biosurfactant. To verify the potential of the biosurfactant for enhanced oil recovery, they constructed a homogeneous, 2D glass micromodel to simulate a post-waterflood biosurfactant injection. 2 PV (pore volumes) of the biosurfactant at CMC concentration levels was injected into the micromodel over the course of two days. At the end of the experiment, they reported that 5% of the OOIP was recovered due to the biosurfactant flooding.

Khaleel (2017) chose to use the rhamnolipid biosurfactant as one of four surfactants in an experiment to determine the most optimal surfactant for use in EOR techniques in carbonate reservoirs. The surfactants were tested to find their optimum salinity, and their IFT was measured at various temperatures, with surfactant concentration at 1% by weight, using a spinning drop tensiometer. The biosurfactant exhibited an IFT of about 0.05 dynes/cm.

Wettability studies were then performed, using discs cut from carbonate cores and determined using contact angle measurements. The rhamnolipid had very little effect on the wettability of the carbonate core disc, changing it from oil-wet at a contact angle of 148.5 at 25° C to just slightly less oil-wet at 96 and 132, at temperatures of 50° C and 75° C respectively.

Gudina, et al. (2015), produced rhamnolipid using low-cost substrates like corn steep liquor and molasses. The bacteria strains were fermented for a total of 144 hours. Once prepared, the produced rhamnolipid was purified, and then freeze-dried to a temperature of -20° C.

Two commercial chemical surfactants were used to compare the performance of the optimized rhamnolipid product in flasks of artificially contaminated sand, which contained 10% of Arabian Light crude oil. The flasks were incubated at 40° C, and the rhamnolipid recovered 55% of the oil at a concentration of 5 mg/mL, while the commercial surfactants recovered 54.4% and 30.5%, respectively, at the same concentration.

Rocha, et al. (1992) recovered two strains of *P. aeruginosa* bacteria from soil samples that were exposed to injection water, produced water, and produced hydrocarbons. Rhamnolipid was produced from the discovered strains and purified. Reactions to salinity, pH factor, temperature, and hardness were measured from the produced biosurfactant at a 1% concentration. The CMC was also determined.

While exact numbers were not reported, the team mention in their work that the two strains “produced stable emulsions of heavy and extra-heavy crude oils” at

temperatures as low as 0° C and as high as 100° C. They also report that the biosurfactant was able to reduce the surface tension of water from 72 to 28 dynes/cm.

Amani (2015b) tested four different surfactants for the purpose of recovering oil from crude oil-contaminated sand. Rhamnolipid, produced from the bacteria strain *P. aeruginosa* PTCC 1310, was one of the four. Another biosurfactant, surfactin, along with two synthetic surfactants, were the other three products tested in this study.

The *P. aeruginosa* was incubated for 72 hours, then extracted and purified. Using a tensiometer, the surface tension was tested and it was found that the produced rhamnolipid reduced the surface tension of water from 72 mN/m to 26 mN/m. The interfacial tension and emulsification index were also tested, with the rhamnolipid achieving the highest emulsification level of 88%, compared with 75%, 70%, and 65% from the other three surfactants respectively.

The rhamnolipid was then added at CMC concentration to sand that was contaminated with 34° API Iranian crude oil at 2.8% by weight, and allowed to work for 24 hours. At both room temperature (25° C) and at 50°C, the rhamnolipid outperformed the other surfactants, recovering 80% at room temperature and 90% at 50° C of the residual oil in the contaminated sand.

In the work of Shafeeq and his team (Shafeeq et. al, 1989), an indigenous strain of *P. aeruginosa* was isolated from coastal waters and tested for use in oil spill clean-up. The surface tension and emulsification index of the produced rhamnolipid product was tested. Due to the emulsification properties of the rhamnolipid, it was found to be very effective

at dispersing oil. The authors recommend that rhamnolipid would be an effective surfactant for use in EOR, as well as for oil spill clean-up purposes.

## 2.2. Alkyl Polyglycosides

In 2009, Iglauer and his team studied the suitability of APG surfactants for EOR applications. Using various types of alcohol as cosurfactants—linear, branched, and cyclic aliphatic alcohols, among others—they tested three types of APG surfactants. Phase behavior tests were performed with the WOR kept at 1. They tested the IFT of the prepared samples using a spinning drop tensiometer, and the effect of varying temperatures was also tested. They found that ultra-low IFT could be created with certain APG-alcohol formulations, reaching as low as 0.001 mN/m. Coreflood tests were then performed using Berea sandstone cores, in which they were able to recover roughly 85% of the OOIP. The tertiary recovery was over 50% of the residual oil within the core.  
(Iglauer et. al, 2009)

A year later, in 2010, Iglauer and his team conducted some further studies using an APG surfactant as well as three others for their potential use in tertiary oil recovery. They performed corefloods on Berea sandstone cores, as well as a sandpack flood in the case of one of the APG/cosolvent formulations. Adsorption tests were performed on kaolinite clay. They performed all of their surfactant formulation steps at atmospheric pressure and ambient temperature, and determined the optimum salinity for the various surfactant mixtures via IFT measurement tests. Their APG formulations recovered 40.8% and 53%

of tertiary oil recovery respectively, with the sandpack flood formulation recovering 94% of the OOIP.

In 2013, Ghosh and Obassi screened several surfactants for use in a carbonate reservoir. The criteria was that the surfactant had to be stable at very high levels of both salinity and temperature, among other things. Because APG is not strongly affected by salinity or temperature levels, various APG surfactants were chosen for their study. Crude oil was obtained from the target field for the experiments, which they filtered and degassed. They based their brine on the composition of the injection water in the same field. Salinity levels as high as 26% were used in their screening tests, with all surfactants tested at a concentration of 1% by weight. Phase behavior studies were performed, along with contact angle measurements and spontaneous imbibition tests. Lastly, they performed coreflooding tests to simulate potential tertiary oil recovery. They found that one of their APG surfactants performed effectively even at the highest levels of temperature and salinity in the experiment, and so concluded that it is a viable surfactant for use in carbonate reservoir EOR techniques.

Yin and Zhang (2013) conducted research on surfactant blends containing APG to test their viability for use in carbonate reservoirs. APG was chosen for the research due to its nontoxic, environmentally friendly nature. Tests on IFT, wettability, and oil displacement efficiency via coreflooding experiments were performed on the APG surfactant and its co-surfactant mixtures. The crude oil used in the testing was obtained from the target field, as were the carbonate cores used in the wettability tests. Synthetic brine was created based on the composition of the formation brine. The IFT experiments were performed using an interfacial tensiometer, and measured at 45° C. The APG

surfactant was able to reduce the IFT to 0.00216 mN/m at a concentration of 0.5% by weight, and was also able to change the rock surface from oil-wet to water-wet in the wettability tests. They also found the surfactant to remain stable at high levels of both salinity and temperature. Overall, it was concluded that APG surfactants are effective for use in EOR processes in carbonate reservoirs.

In the work of Santa and her team (2011), a study was performed to find sustainable surfactants for EOR techniques. They compared various types of APG surfactants using phase behavior tests and IFT measurement tests. Crude oil and decane were used in their tests as the oil phase components, and they used 1-octanol as a co-solvent in the phase behavior studies.

High levels of salinity, hardness, and temperature were used to test the stability of the surfactants, with the highest values being 18% salinity, with 13,600 ppm of  $\text{Ca}^{2+}$  and 2100 ppm of  $\text{Mg}^{2+}$ , and 80°C. Only those that remained stable for three days were used for further testing. They found that short-chain and mid-chain APG surfactants performed best under extreme conditions.

The interfacial tension tests were performed using a spinning drop tensiometer, using surfactant concentrations of 0.2% by weight. Salinity levels were varied, with tests performed at 5%, 10%, and 18%. The temperature was varied as well, with measurements taken at 20°, 50°, and 70° C. They found that the alcohol chain length and the hydrophilic/lipophilic balance (HLB) strongly affected the IFT results between the various surfactants. They also found that stable microemulsions could be formed when the APG surfactants are combined with a co-solvent.

## 2.4. Lecithin

Nguyen and his team (Nguyen, et al., 2010) used lecithin, rhamnolipid, and sophorolipid, another biosurfactant, to form solvent-free microemulsions using five different types of oils with different EACN values. All of the lecithin-containing mixtures were able to form middle phases with the different oils, as well as achieving ultra-low IFT values. They were also found to be stable at a variety of temperatures and salinity levels.

Ojukwu and his team (Ojukwu, et al., 2013) used lecithin as an EOR surfactant for recovering crude oil from sand packs. The sand packs were first saturated with brine, then with oil. To simulate secondary recovery, the sand pack was flooded with brine until oil ceased to flow, and then the lecithin surfactant was used in a surfactant flood for tertiary recovery. It was found that lecithin alone was able to recover 25% of the original oil in place.

In 2015, Riehm and his team (Riehm et al., 2015) tested the effectiveness of a lecithin-containing formulation for dispersion of crude oil in synthetic sea water, searching for a greener way of treating oil spills. The mixture was formulated using lecithin, a second surfactant, and a solvent in which the two surfactants were dissolved. They tested their formulation using baffled flask tests containing synthetic sea water and crude oil at dispersant-to-oil ratios (DOR) ranging from 1:25 all the way up to 1:100. They found that their formulation was 89% effective at a DOR of 1:25 and remained highly effective even at a DOR of 1:100, achieving 77% dispersion.

Nouraei and Acosta (Nouraei & Acosta, 2017) used the HLD concept to determine the characteristic curvature ( $C_c$ ) of soybean lecithin for the purpose of creating a fully dilutable microemulsion ( $\mu$ Es), which they then used to design a self-microemulsifying delivery system (SMEDS). They introduced the idea of using the HLD concept to formulate dilutable  $\mu$ Es, rather than the trial and error approach generally used today. After obtaining the  $C_c$  of the soybean lecithin and the other components of their system, they performed salinity scans to study the phase behavior. They found that lecithin was highly effective at solubilizing the oil and water in their microemulsion system.

Rocchio and his team (Rocchio, et al., 2017) used lecithin as a component in a two-surfactant formulation used to disperse both gasoline and crude oil in synthetic sea water, as part of a bioremediation study. They found that their formulation was able to emulsify both the gasoline and the crude oil at greater than 90% emulsion efficiency. They also found that surfactant mixtures containing lecithin can create effective coatings that prevent oil deposition to hydrophobic surfaces, giving bird feathers as an example.

## 2.5. Summary and Knowledge Gap

A summary of the literature survey in tabular form is included in Appendix A. As can be noted from much of the above literature, green surfactants are beginning to gain popularity for their potential in EOR. However, the research in this area is still in its early stage and further studies are required to fully understand and utilize the potential of green surfactants. Some of the limitations of the currently published literature regarding the two green surfactants that will be utilized in this study are:

- Rhamnolipid has never been studied for effectiveness in sandstone core-flood EOR experiments. Most of the studies performed on rhamnolipid are aimed at bioremediation techniques in contaminated soil, sand, and seawater. The efficient IFT-lowering properties of rhamnolipid can also lend themselves well to chemical EOR processes, and this possibility should be tested and exploited.
- Surfactant formulations using rhamnolipid as the primary surfactant have not been attempted, nor have there been tests using rhamnolipid with a cosolvent alcohol. Either of these options may produce a very effective chemical mixture for use in EOR chemical floods.
- While APG surfactants have been widely studied for uses such as laundry detergents and cleaning formulas, there are relatively few studies focusing on APG as a possible surfactant for EOR, and even fewer attempting to test the potential of APG in sandstone reservoirs.

## CHAPTER THREE - METHODOLOGY

### 3.1. Materials

The crude oil used in the study was Arabian crude with an API of 30° and an EACN of 11. The other materials used are listed below.

Material	Purity	Supplier	Role
Anionic biosurfactant, Rhamnolipid	90%	AGAE Tech.	Primary surfactant
Nonionic green surfactant, APG Glucopon® 600 CSUP	50- 75%	BASF Corp.	Cosurfactant
1-Butanol	99%	Sigma- Aldrich	Cosolvent
Lecithin	97%	Fearn	Cosurfactant
NaCl (Sodium Chloride)	99.5%	Sigma- Aldrich	Synthetic brine

Table 2 - List of materials

## 3.2. Phase Behavior Study

### 3.2.1. Introduction

Phase behavior refers to the interactions between various homogeneous parts of a given system. Each phase in the system is physically distinct and separate from the other parts of the system, even as they are in contact with one another (Ahmed, 2007). In surfactant flooding, the system consists of brine, surfactant, and oil. The phases are aqueous and oleic, with the surfactant expected to blur the boundary between them, lowering the interfacial tension.

This surfactant behavior is the core of phase behavior tests for enhanced oil recovery purposes. Under the right conditions, the surfactant micelles are able to solubilize the crude oil in the system to form a stable phase known as a microemulsion. A microemulsion can be transparent or translucent, and it is both isotropic and thermodynamically stable (Sheng, 2011).

Phase behavior is strongly affected by salinity level. Higher salinity levels generally decrease the solubility of anionic surfactants in the brine, and moves the surfactant from the aqueous phase to the oleic phase.

Winsor (1954) reported a number of phase behaviors that a surfactant-oil-brine system might display. In a Winsor type I system, also known as a type II(-), the surfactant is in the aqueous phase with crude oil solubilized within the micelles, creating a lower phase microemulsion. This phase is often found in lower salinity environments. The

Winsor type II, or type II(+), is often found at high salinity levels. The surfactant is in the oleic phase, with solubilized brine contained within the micelles. The phase that is considered to be ideal for EOR purposes is the Winsor type III, also known as a middle phase microemulsion. In this type of microemulsion, there are separate excess oil and water phases, with the microemulsion formed in between them. This type is of interest in EOR because it is known to correspond to ultralow IFT values. **Figure 1** demonstrates the three types using ternary diagrams.

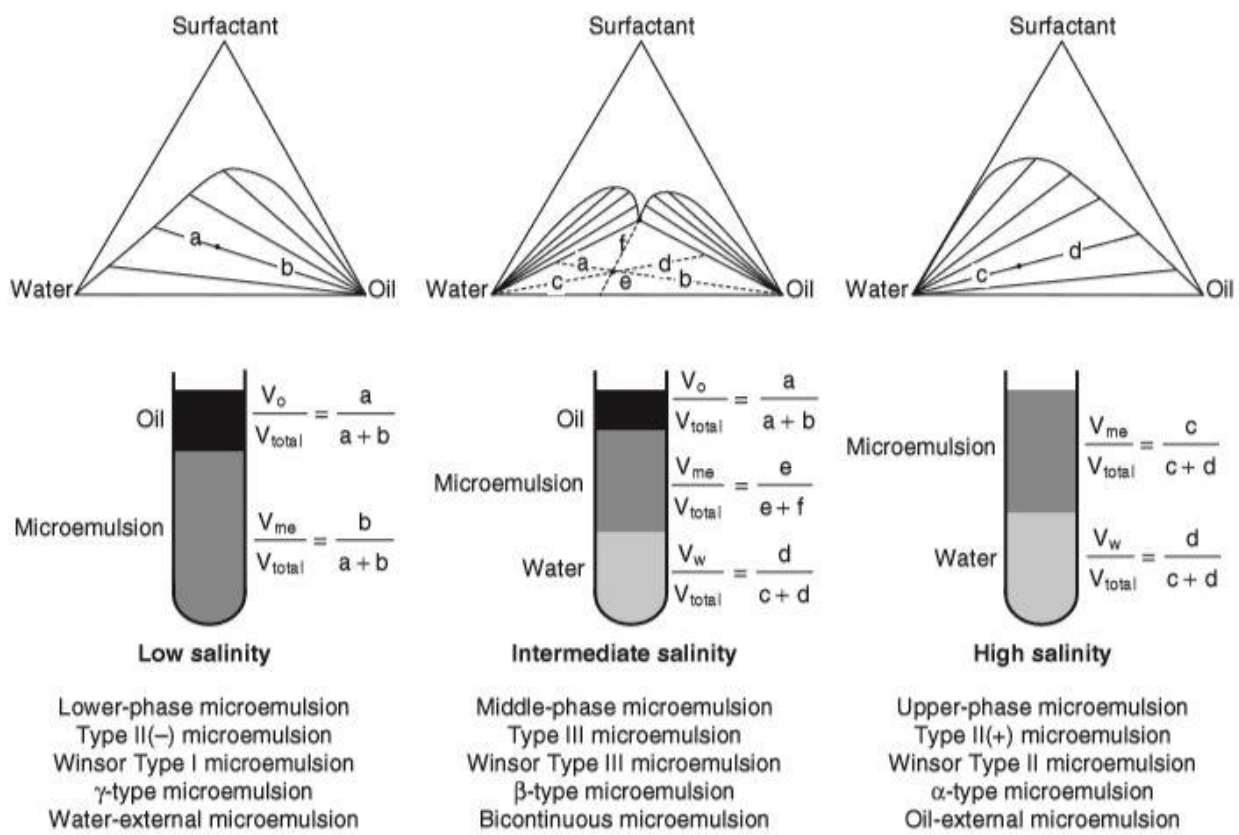


Figure 1 – Microemulsion phase types. Taken from the work of Sheng (2011)

### 3.2.2. Background

The phase behavior of a surfactant/oil/brine system is quite complex. One source of complexity is due to the large number of variables that can alter the behavior of the system. Salager (Salager, et al., 1979) categorized these variables into three groups:

- 1) Formulation variables are those factors related to the components of the system such as the surfactant structure, oil carbon number, salinity and alcohol type and concentration.
- 2) External variables are factors related to the environment in which the system is studied, like the temperature and the pressure.
- 3) Position variables, such as the surfactant concentration and the water-oil ratio (WOR). He used the term position variables because knowledge these variables is required to locate the system in a ternary diagram.

In his study, he showed that the optimum formulation, one that will result in Winsor Type III, is obtained whenever a certain condition or correlation is satisfied between the formulation variables. For anionic surfactants, the relationship has been expressed as (Salager, et al., 1979):

$$\ln S - K(ACN) - f(A) + \sigma - a_T \Delta T = 0$$

For nonionic surfactants, a similar correlation was found (Bourrel, et al., 1980):

$$\beta + bS - K(ACN) - \Phi(A) + c_T \Delta T = 0$$

In these expressions:

- S is the salinity expressed as (NaCl g/100mL).
- ACN is the alkane carbon number, a characteristic parameter for the oil phase.
- $f(A)$ ,  $\Phi(A)$  are functions of the alcohol type and concentration
- $\sigma, \beta$  characteristic parameter for structure of the surfactant.
- $EON$  is the average number of ethylene oxide group per molecule of non-ionic surfactant.
- $\Delta T$  is the temperature deviation measured from a certain reference ( $25^\circ\text{C}$ ).
- $K, b, a_T$  and  $c_T$  are empirical constants.

When the oil phase is a simple alkane, the ACN is simply the number of carbon atoms. For oil phases that are a complex mixture of different types of oils, the concept of Equivalent Alkane Carbon Number (EACN) is used to represent the oil phase in the correlation. The EACN enables us to model the interfacial tension behavior of a complex oil mixture with a single number as if it was a simple alkane (Cayias, et al., 1976). For example, Decalin behaves like an alkane possessing six carbon atoms even though it has ten (Cash, et al., 1977). The EACN of an oil mixture can be computed from its composition by a linear mixing rule based on molar fraction.

In subsequent years, it was established that this correlation was a numerical expression for the surfactant affinity difference, known as SAD (Salager, et al., 2013). SAD is the difference between the negative of the standard chemical potential of the surfactant in the oil phase and the corresponding term for the water phase expressed mathematically as:

$$SAD = \mu^{*W} - \mu^{*O}$$

Where  $\mu^*$  is the standard chemical potential at some reference condition. SAD measures the standard chemical potential change during the transfer of a surfactant molecule from the oil to the water phase. To obtain a dimensionless form:

$$\frac{SAD}{RT} = HLD$$

Where HLD is the hydrophilic–lipophilic deviation from an optimum formulation. It is a measure of the imbalance of the surfactant between the phases and its expression was found to be identical to the correlation presented by Salager (Salager, et al., 1979):

$$HLD = \frac{SAD}{RT} = \ln S - K(ACN) - f(A) + \sigma - a_T \Delta T \text{ for ionic surfactants}$$

and

$$HLD = \frac{SAD}{RT} = \beta + bS - K(ACN) - \Phi(A) + c_T \Delta T \text{ for nonionic surfactants}$$

### 3.2.3. Experiments

The phase behavior of various green surfactant formulations that have been developed using the HLD concept were tested in this part of the study using salinity scans. The Cc of the surfactants were obtained from the literature to begin with, and their final numbers were determined from the results of preliminary scans. Concentration of the surfactant, cosurfactant, and cosolvent were fixed, the salinity was varied in increments of 1%, with the range of the salinity scan depending on the type of formulation and the

calculated HLD value of the blend. A number of salinity scan tests were conducted, using various surfactant/cosurfactant/cosolvent formulations. In all cases, the WOR (water-oil ratio) were kept at 1.

Set Name	Salinity wt%	Surfactant wt%	Cosurfactant wt%	Co-solvent wt%	Oil Type
RB	1-20%	Rhamnolipid - 1%	0%	3% 1-butanol	Crude
RAB	1-10%	Rhamnolipid - 1%	APG - 1%	3% 1-butanol	Crude
RL	1-16%	Rhamnolipid - 2 %	Lecithin – 2%	0%	Crude

*Table 3 - List of optimized formulations and their salinity scan variations*

The volume of the oil and the water were measured at 5 mL each, causing half of the sample to be in the oil phase, and half to be in the aqueous phase, which consisted of brine of varying salinity mixed with the surfactant solution. For maximum accuracy and precision, graduated pipettes were used to measure out each individual component.

The surfactant mixtures were prepared using weight percent, with each component being added by weight instead of volume. They were mixed thoroughly using a vortex spinner until all the components were completely dissolved, then added into glass test tubes using graduated pipettes. The crude oil was then added, also with the use of graduated pipettes, and each of the tubes were thoroughly shaken by hand for 30 seconds.

After shaking, the mixture was left to stabilize and reach equilibrium at room temperature. Equilibrium can be considered to have been achieved if there have been no further changes in the various phase volumes over 24 hours (Haq, 2012). The mixtures were monitored carefully for changes over several days, and the final phase volumes were then recorded and used to calculate the solubilized volumes of oil and water based on the difference between the initial and final volumes of each phase.

### 3.3. Fluid Properties Tests

The methodology and equipment used to measure fluid properties including density, viscosity, and interfacial tension (IFT) are described in this section.

#### 3.3.1. Sample Preparation

For the density and IFT measures, three sets of samples were prepared. Each set represented one of the three formulations that were chosen after the phase behavior study.

- Set A contained rhamnolipid as the primary surfactant and 1-butanol as the co-solvent alcohol. The concentration ratio of rhamnolipid to butanol was set at 1:3, matching the concentration ratio used in the phase behavior study.
- Set B consisted of rhamnolipid as the primary surfactant, APG as the cosurfactant, and 1-butanol as the co-solvent alcohol. The concentration ratio of the three components was set to 1:1:3, matching the concentration used in the phase behavior study.
- Set C consisted of rhamnolipid as the primary surfactant and lecithin as the cosurfactant with a concentration ratio of 1:1.

The concentration of the rhamnolipid was increased in 0.02 wt.% increments for the first four samples in each set, with the last sample having the same concentration as the one used in the phase behavior study. The following tables contain the data for each of the three sets.

Sample	Rhamnolipid Concentration (wt.%)	1-Butanol Concentration (wt.%)
A1	0.02	0.06
A2	0.04	0.12
A3	0.06	0.18
A4	0.08	0.24
A5	0.5	1.5

Table 4 - Surfactant and co-solvent concentration data for set A

Sample	Rhamnolipid concentration (wt.%)	APG concentration (wt.%)	1-butanol concentration (wt.%)
B1	0.02	0.02	0.06
B2	0.04	0.04	0.12
B3	0.06	0.06	0.18
B4	0.08	0.08	0.24
B5	0.5	0.5	1.5

Table 5 - Surfactant, cosurfactant, and co-solvent data for set B

Sample	Rhamnolipid Concentration (wt.%)	Lecithin Concentration (wt.%)
C1	0.02	0.02
C2	0.04	0.04
C3	0.06	0.06
C4	0.08	0.08
C5	0.25	0.25

Table 6 - Surfactant and cosurfactant concentration data for set C

### 3.3.2. Density Measurements

The density of the crude oil, brine and the surfactant formulations at different concentrations was measured at both room temperature and at typical reservoir temperature (25° and 52° C, respectively). Density values are required for measurement of the interfacial tension between the oil and the surfactant formulations when using the spinning drop tensiometer method for IFT measurement.

### 3.3.2.1. Apparatus

The density values were measured using a densitometer (DMA 4500, Anton Paar). This apparatus measures density using the oscillating U-tube method by measuring the oscillating frequency and converting it into a density value. An image of the device is shown in **Figure 2**.



Figure 2 - DMA 4500 Anton Paar Densitometer

### 3.3.2.2 Procedure

The following steps were carried out:

1. The measuring tube was cleaned with distilled water and was then dried using a pump drier.
2. The calibration of the equipment was checked by measuring the density of distilled water.
3. The sample was injected into the densitometer using a syringe.
4. The required temperature was set.
5. The density value was recorded.

### 3.3.3. Viscosity Measurements

The viscosity of a fluid is an important parameter in the study of petroleum fluid flow in reservoirs. It is a measure of the resistance of a fluid to flow. Viscosity,  $\mu$ , is sometimes called dynamic viscosity to distinguish it from kinematic viscosity. The kinematic viscosity,  $\nu$ , of a fluid is a measure of the resistance of the fluid to flow under the influence of gravitational force. It is related to dynamic viscosity by the following equation:

$$\nu = \frac{\mu}{\rho}$$

Where:

- $\nu$  is kinematic viscosity in centistoke (cSt).

- $\mu$  is dynamic viscosity in centipoises (cP)
- $\rho$  is the density of the fluid in g/cm<sup>3</sup>

The viscosity of the crude oil and the brine was measured at both room and reservoir temperatures (25° and 52° C, respectively).

#### 3.3.3.1. Apparatus

The viscosity was measured using a U-tube viscometer (also known as an Ostwald viscometer) which was immersed in the thermostatic visibility bath shown in **Figure 3** (TV4000, Tamson Instruments). The viscometer operates on the principle that the time a fixed volume of liquid takes to flow from one point to another is proportional to the kinematic viscosity of the fluid, i.e.:

$$\nu \propto t$$

or

$$\nu = ct$$

Where:

- $c$  is the viscometer constant (est/sec).
- $t$  is the time (sec).



Figure 3 - Tamson TV4000 thermostatic visibility bath

### 3.3.3.2. Procedure

The following steps were carried out:

1. A viscometer size was selected based on the estimated viscosity of the fluid.
2. The viscometer was cleaned with distilled water and dried.
3. The viscometer was filled with the liquid for which the viscosity will be measured.
4. The viscometer was inserted into the thermostatic bath.
5. The desired temperature was set.
6. The liquid sample was sucked to the first marker and then allowed to flow under its own weight.
7. The time taken for the fluid to pass between the two markers was recorded using a stop watch.
8. The dynamic viscosity was calculated.

### 3.3.4. Interfacial Tension Measurements

#### 3.3.4.1 Introduction

Interfacial tension (IFT) is the measure of the tension at the face of two distinct fluids that are in contact with each other, such as oil and water. Lowering the IFT between formation water and residual oil is an essential part of the enhanced oil recovery process,

and the measurement of the IFT is one of the most important fluid property tests that must be done when performing surfactant floods. If a surfactant cannot successfully lower the interfacial tension between the aqueous and oleic phases commonly found in a reservoir (crude oil and brine), it will not be successful in producing the trapped oil remaining in the reservoir.

The interfacial tension can be correlated with the capillary number, which is a dimensionless quantity that represents the ratio of the viscous forces attempting to displace the residual oil to the capillary forces attempting to trap the oil in place. In order to mobilize the residual oil and move it towards the production well, the capillary number must be increased significantly. One of the most effective ways to achieve this is to reduce the interfacial tension to an ultralow value of around  $10^{-3}$  mN/m. The mathematical representation of the capillary number is given by:

$$N_c = \frac{v\mu}{\gamma}$$

Where:

- $N_c$  = the capillary number
- $v$  = interstitial velocity
- $\mu$  = viscosity
- $\gamma$  = the interfacial tension between the crude oil and the displacing fluid

The optimum concentration of any given surfactant or biosurfactant is determined by the CMC, or critical micelle concentration. After the CMC is reached, the IFT decreases are often negligible with further additions of surfactant into the mixture, making the optimum concentration just under the CMC level. So, to determine the CMC of the

various surfactant formulations, we will calculate the results from the IFT measurement tests and plot them against the surfactant concentration levels in each individual test.

#### 3.3.4.2. Apparatus

A spinning drop tensiometer (*M6500, Grace Instrument Company*) was used to measure the interfacial tension. An image of the apparatus can be seen in **Figure 4**.



Figure 4 - M6500 Spinning Drop Tensiometer.

#### 3.3.4.2.1. Working Principle

To measure the interfacial tension between two fluids, a heavy bulk phase and a light drop phase are placed into a rotating capillary. The rotation of the capillary elongates the drop, with the shape of the drop stabilizing when the interfacial tension and centrifugal forces are balanced. This is known as the equilibrium point, and it is at this point that the interfacial tension can be calculated from the measured drop diameter, using the following equation:

$$\gamma = \frac{r^3 \omega^2 (\rho_H - \rho_L)}{4}$$

Where:

- $\gamma$  = the interfacial tension between the phases
- $r$  = the radius of the drop
- $\omega$  = the angular frequency of the capillary rotation
- $\rho_H$  = density of the bulk phase
- $\rho_L$  = density of the drop phase

To analyze the drop shape, the apparatus illuminates the drop from one side and records it with a camera from the opposite side. The accompanying software determines the drop diameter from the image obtained from the camera.

#### 3.3.4.3. Procedure

The following steps were carried out:

1. The capillary tube was cleaned with distilled water and rinsed with the sample.
2. The sample was injected until the capillary tube is full.
3. Using a syringe, a drop of crude oil was injected.
4. The capillary tube was checked for the presence of air bubbles. If present, the previous steps were repeated.
5. The desired temperature was set and allowed to equilibrate.
6. The Angular Frequency (RPM) was between 3000 and 8000 to ensure that the drop length is be at least four times the diameter, and the drop outlines are not curved.
7. The measurement of the dimeter of the oil drop was recorded from the software.
8. The experiment was carried out for 30 minutes and IFT value at the end of that period was calculated.

### 3.4. Core-Flooding Tests

#### 3.4.1. Introduction

In this section, core-flooding experiments are performed to attempt to discover the likely behavior of a given surfactant inside of a reservoir under common reservoir pressure and temperature levels. The amount of oil recovered by a given surfactant during a core flood can give a good indication of the possible tertiary recovery under normal reservoir conditions. We will be performing three core flood tests using the surfactant formulations that displayed the lowest IFT values in the previous fluid properties study.

### 3.4.2. Apparatus

The core flooding experiments were conducted using a FDES-645Z from Coretest Systems, Inc. **Figure 5** is a picture of the system with a brief description of the main components, and **Figure 6** displays the components that reside inside the oven along with a short description of each. A gas cylinder was connected to the BPR gas supply connection to provide the backpressure for the system. In addition, a pump (from Teledyne-Isco) is used to provide the confining pressure inside the core holder.

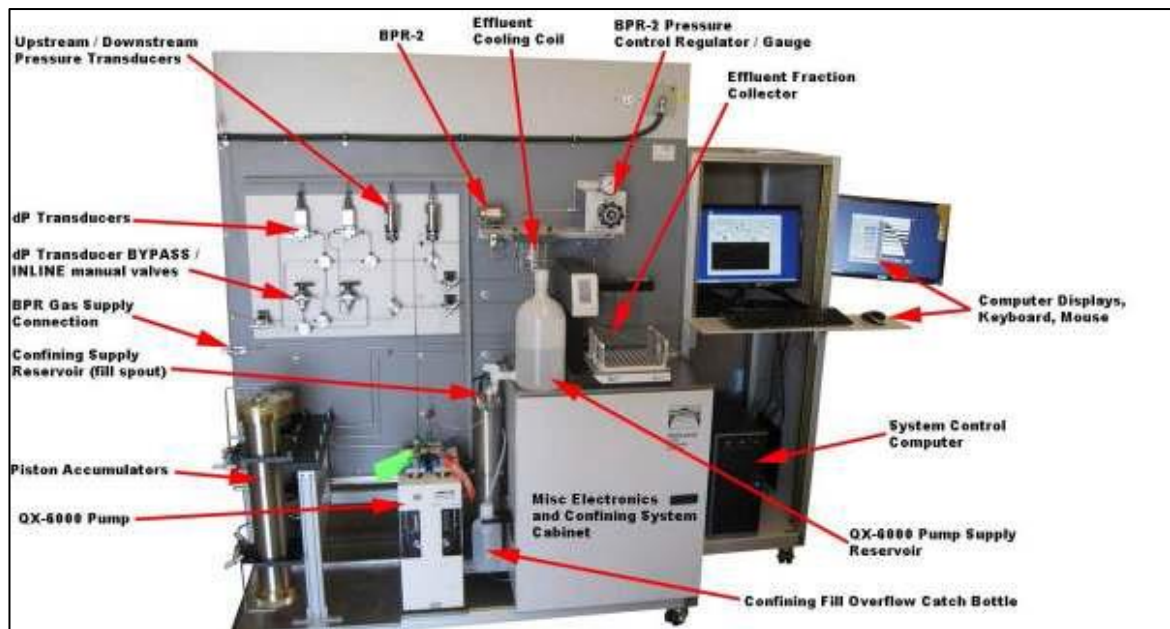


Figure 5 - FDES-645Z core-flooding apparatus



Figure 6 - FDES-645Z core-flooding apparatus, inside-oven view

### 3.4.3. Procedure

The steps that were followed in performing the three core flooding experiments are recorded below in detail.

#### 3.4.3.1. Core Sample Preparation

1. The core samples were obtained from Berea sandstone rock. Berea was chosen because it is a standard representative for sandstone in porous laboratory experiments in the petroleum industry and in the literature.
2. Three cores measuring 1.5 inches in diameter and 6 inches in length were cut.
3. The dry cores were weighed, and their length and diameter were measured.

#### 3.4.3.2. Brine Saturation

1. A 3 wt.% NaCl brine solution was prepared by adding the required amount of sodium chloride to distilled water. The solution was stirred using a magnetic stirrer until the salt was completely dissolved.
2. The core was placed in the core holder.
3. A vacuum pump was connected to one end of the core holder and a vacuum was applied to the core to remove air trapped within the core and to ensure that the core would be fully saturated with brine.

4. A pump was connected to the inlet end of the core holder and a pressure gauge was connected to measure the pressure inside the core holder.

5. Brine was pumped into the core until the pressure inside the core holder was around 2000 psi.

6. The pump was disconnected from the core holder and the isolated core holder was left for 24 hours.

7. After the 24 hours had passed, the core was removed from the core holder. It was assumed that the core was fully saturated with brine at this point.

8. The wet core surface was gently wiped with paper to remove water from the surface of the core sample.

9. The brine-saturated core weight was measured, and the porosity of the core was calculated.

10. The core sample was wrapped in aluminum foil to preserve the saturated core until the start of the core-flooding portion of the experiment.

#### 3.4.3.3. Loading the Core into the Apparatus

1. The core sample and appropriately sized spacers were inserted into a rubber sleeve, which was then inserted at one end of the core holder. The sleeve grips and squeezes the core when confining pressure is applied and ensures that the flow goes through the core sample and not around it.

2. The fixed-end end cap was tightly screwed.

3. The variable-end end cap was tightened until pressure was applied on the face of the core sample.

4. The core holder was loaded into the system and the tube for the confining pressure was connected.

5. A confining pressure of 1000 psi was applied and the system was monitored for any leaks from the ends of the core holder.

6. The inlet and outlet tubes were connected.

#### 3.4.3.4. Charging the Accumulators

The system contains four accumulators, two inside the oven chamber and two outside. These accumulators were cleaned, and one of the accumulators in the oven chamber was filled with the crude oil while the two accumulators on the outside were filled with the brine and the surfactant solution, respectively.

#### 3.4.3.5. Absolute Permeability Determination

1. The flow valves that permit the flow of fluids from the accumulator to the core were closed.

2. The flow valve that permits the flow of brine from the brine accumulator to the core was opened.

3. The pump that drives the fluids from the accumulator to the core was started at a rate of 5 mL/min.

4. The back-pressure was incrementally increased until it reached a value of 1000 psi.
5. The confining pressure was also raised incrementally at the same time until it reached a value of 2000 psi.
6. The oven temperature was raised to 52° C.
7. The pressure of the system was monitored to ensure that there were no leaks in any of the tubes or the connections.
8. For permeability determination, the rate was started at 4 mL/min until the pressure stabilized. Once pressure stabilization was reached, the pressure difference value was recorded.
9. The previous step was repeated at the rates of 3 mL/min, 2 mL/min and 1 mL/min.
10. The rate was then set to 0.5 mL/min, and flow continued until the pressure stabilized.
11. The absolute permeability of the brine-saturated core was calculated.

#### 3.4.3.6. Crude Oil Saturation

1. The flow valve that permits the flow of brine from the brine accumulator to the core was closed.
2. The flow valve that permits the flow of crude oil from the crude oil accumulator to the core was opened.

3. The injection rate was set 0.5 mL/min and the produced brine and oil were collected in a graduated cylinder.
4. The crude oil injection was continued until there was no water observed in the effluent.
5. The pressure at the inlet and outlet of the core was recorded to calculate the effective oil permeability at residual water saturation.
6. The flow valve for the oil accumulator was closed and the pump stopped.
7. The volume of the brine collected, minus the dead volume held inside the tubes, was used to calculate the residual water saturation.

#### 3.4.3.7. Waterflooding

1. The core was left to age at the previously specified pressure and temperature conditions for a minimum of 48 hours.
2. After completion of the aging process, the flow valve for the oil was opened and the pump was started at a rate of 0.5 mL/min until the pressure stabilized.
3. After the pressure stabilized, the flow valve for the oil was closed and the one for brine was opened.
4. The produced brine and oil were collected in 10 mL graduated tubes.
5. The waterflood continued until negligible amounts of oil were produced.

#### 3.4.3.8. Surfactant Flooding

1. The flow valve for the brine was closed and the one for the surfactant was opened.
2. The produced fluids were collected in 10 mL graduated tubes.
3. The surfactant flood continued until a negligible amount of oil was being produced or 3 pore volumes of surfactant had been injected.

#### 3.4.3.9. Brine Post-Flush

1. The flow valve for the brine was opened and the one for the surfactant was closed.
2. The produced fluids were collected in 10 mL graduated tubes.
3. The brine post-flush continued until a negligible amount of oil was being produced or 3 pore volumes of brine had been injected.

### 3.5. Simulation of Core-Flooding Experiment

#### 3.5.1 Introduction

As the interest in chemical enhanced oil recovery increased and the application of its techniques have become popular both in the laboratory and field settings, it was apparent that conventional reservoir simulators were not equipped to fully model the

unique aspect of this recovery process. This has prompted several research centers and companies to develop a solution that can provide the advanced modelling capabilities required to simulate it. STARS, ECLIPSE and UTCHEM are among the most widely used simulators to model chemical enhanced oil recovery processes.

In this part of the study, a commercial reservoir simulator (Eclipse) is used to model the surfactant core flooding experiments. A three-dimensional Cartesian model having the same volume as the cores is constructed; rectangular grids are used to simplify the modeling process. The fluid properties for the surfactant formulations, along with those of the oil and brine, are incorporated into the model. Oil recovery from the waterflooding and surfactant flooding phases is then generated by running the simulation model, and the results are compared to those obtained during the core flooding experiments.

### 3.5.2 Background

Reservoir simulation is a form of numerical modeling used to quantify and interpret physical phenomena with the capability to extend these phenomena to predict future performance. The process involves dividing the reservoir into several discrete units in three dimensions, and modeling the change of reservoir and fluid properties through space and time in a series of discrete time-steps.

The equation solved for each cell and for each time-step is a combination of Darcy's Law and the material balance equation. Darcy's Law is an empirical relationship

between fluid flow rate through a porous medium and the potential gradient. It can be expressed as:

$$u = \beta_c \frac{k}{\mu} \nabla \Phi$$

Where:

- $u$  is the superficial velocity
- $k$  is the permeability
- $\mu$  is the viscosity
- $\Phi$  is the fluid potential
- $\beta_c$  is a unit conversion factor

The definition of the potential gradient is:

$$\nabla \Phi = \nabla p - \gamma \nabla Z$$

Where:

- $Z$  is the elevation.
- $p$  is the pressure.
- $\gamma$  is the fluid gravity defined by  $\gamma = \gamma_c \rho g$
- $\rho$  is the density
- $\gamma_c$  is a gravity conversion factor
- $g$  is acceleration due to gravity

The material balance equation for a single-phase flow for 3D rectangular flow can be expressed as:

$$-\frac{\partial}{\partial x}(\dot{m}_x A_x) \Delta x - \frac{\partial}{\partial y}(\dot{m}_y A_y) \Delta y - \frac{\partial}{\partial z}(\dot{m}_z A_z) \Delta z = V_b \frac{\partial}{\partial t}(m_v) - q_m$$

Where:

- $A_x, A_y, A_z$  are the cross-sectional area normal to the x, y, or z direction
- $t$  is time
- $V_b$  is the bulk volume, control volume, or gridblock bulk volume.
- $q_m$  is mass production rate
- $x, y, z$  is the distance in the x, y, or z direction in Cartesian coordinate system
- $\Delta x, \Delta y, \Delta z$  is the difference along the x, y, or z direction
- $m_v$  is mass per unit volume of porous media at time  $t$
- $\dot{m}_x, \dot{m}_y, \dot{m}_z$  is the x, y, or z component of mass flux vector defined by:

$$\dot{m}_x = \alpha_c \rho u_x$$

Where:

- $\dot{m}_x$  is the x component of mass flux vector
- $\alpha_c$  is a volume conversion factor
- $\rho$  is the density
- $u_x$  is the volumetric velocity in the x direction

By combining the Darcy's Law and material balance equations, the flow equation for a single phase can be obtained. The flow equation can be expressed in the following form for single-phase flow:

$$\begin{aligned} \frac{\partial}{\partial x} \left[ \beta_c \frac{k_x A_x}{\mu_l B_l} \left( \frac{\partial p}{\partial x} - \gamma_l \frac{\partial Z}{\partial x} \right) \right] \Delta x + \frac{\partial}{\partial y} \left[ \beta_c \frac{k_y A_y}{\mu_l B_l} \left( \frac{\partial p}{\partial y} - \gamma_l \frac{\partial Z}{\partial y} \right) \right] \Delta y \\ + \frac{\partial}{\partial z} \left[ \beta_c \frac{k_z A_z}{\mu_l B_l} \left( \frac{\partial p}{\partial z} - \gamma_l \frac{\partial Z}{\partial z} \right) \right] \Delta z = \frac{V_b}{\alpha_c} \frac{\partial}{\partial t} \left( \frac{\varphi}{B_l} \right) - q_{lsc} \end{aligned}$$

Where:

- $A_x, A_y, A_z$  is the cross-sectional area normal to the x, y, or z direction
- $B_l$  is the formation volume factor of Phase  $l$
- $k_x, k_y, k_z$  is the permeability in the direction of the x, y, or z axis
- $l$  is a subscript referring to phase type; can be water, oil, or gas
- $p$  is the pressure
- $q_{lsc}$  is the production rate of Phase  $l$  at standard conditions
- $t$  is the time
- $V_b$  is the bulk volume, control volume, or gridblock bulk volume
- $x, y, z$  is the distance in the x, y, or z direction in Cartesian coordinate system
- $Z$  is the elevation
- $\Delta x, \Delta y, \Delta z$  is the difference along the x, y, or z direction,
- $\alpha_c$  is the volume conversion factor
- $\beta_c$  is the transmissibility conversion factor
- $\gamma_l$  is the gravity of Phase  $l$
- $\mu_l$  is the viscosity of Phase  $l$
- $\varphi$  is the porosity

Eclipse 100 is utilized to simulate the core flooding process for the three surfactant formulations. It is a black oil simulator that employs the finite difference approach to solve a combination of the Darcy's Law and material balance equations for each cell at every time-step. It operates under the assumption that oil and gas phases can each be represented as one component through time, and that only their properties and not their composition can change with pressure and temperature.

### 3.5.3 Input Format

The input model to Eclipse is provided in the format of a text file, with a DATA file extension type. In this file, all of the model information is specified. The file is divided into eight sections, each of which is introduced by a keyword. In each section, keywords can be used to identify input data, request output data, or specify conditions.

The first section, which is identified by the RUNSPEC keyword, is used to specify general model characteristics such as the title, dimensions of the model, active phases present, unit convention, and start date for the simulation. It is followed by the GRID section, where the basic geometry of the simulation grid and various rock properties are specified. The third section is identified by the EDIT keyword. It is an optional section where modifications to the processed GRID section data can be detailed. The fourth section is marked by the PROPS keyword. In this section, the rock and fluid pressure-dependent properties are specified in multi-tabular format. The fifth section, which is an optional section marked by the REGIONS keyword, is used to specify the subdivision of the reservoir. The next section is identified by the SOLUTION keyword. In this section,

the initial state of the model can be set by defining the initial pressure, saturations, or compositions for every grid block. The seventh section, marked by the SUMMARY keyword, is an optional section used to specify output to be written to Summary files at the end of each time step. The eighth and last section, which is identified by the SCHEDULE keyword, is used to specify operations to be simulated and the times at which the output reports are required.

### 3.5.4 Model Description

The cores were modeled using a three-dimensional Cartesian rectangular grid. The grids consist of one layer and were divided into 10 cells in the x direction. An example can be seen in **Figure 7**. The dimensions of the cells were selected so that the volume of the model would be the same as the volume of the core. The dimensions of the cells and the overall volume of the model are specified in **Table 7**.

Exp. #	Cell Length (cm)	Cell Width (cm)	Cell Height (cm)	Model Volume (cm <sup>3</sup> )	Core Volume (cm <sup>3</sup> )
1	1.52	3.367	3.367	172.385	172.39
2	1.51	3.367	3.367	171.234	171.25
3	1.49	3.367	3.367	168.983	168.98

*Table 7 - Cell and simulation model dimensions*

To simulate the injection and production from the two ends of the core, an injection well was placed at the first cell and a production well was placed at the last cell. The two wells were perforated throughout the core thickness with a wellbore diameter of 1 cm. Both wells were controlled using a fixed liquid rate constraint of 0.5 cc/min, which is the same rate that was used during the core flooding experiments.

The rock and fluid properties required for the simulation runs were obtained from the previous IFT and core flooding experiments. Default or assumed values were used for properties that were not measured in the experimental part of this study. The input data for all three formulations can be found in Appendix B.

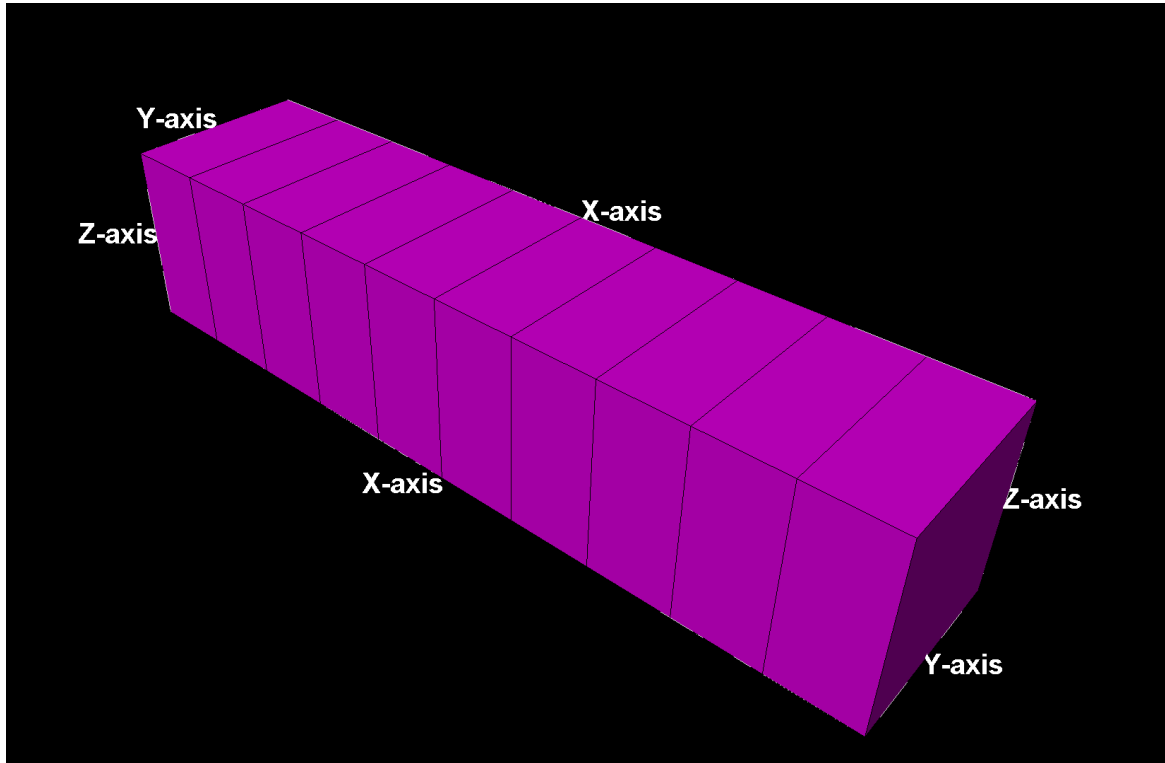


Figure 7 – Modeled three-dimensional Cartesian rectangular grid

# 4

## CHAPTER FOUR - RESULTS AND DISCUSSION

### 4.1. Phase Behavior Study

Test tubes samples were prepared with 5 mL of the relevant aqueous surfactant formulation and 5 mL of crude oil. The salinity of the aqueous solution was varied in increments of 1%. The tubes were mixed thoroughly. Afterwards, they were left for 48 hours or more to allow the fluids to reach phase equilibrium in ambient temperature and pressure. The phase characteristics of each system were recorded. These were the relative volume of the aqueous phase, the middle phase, and the oleic phase.

The objective of the phase behavior study was to test if the proposed formulation would develop a middle phase region. It has been established that low IFT values are obtained when a middle phase microemulsion is formed (Healy & Reed, 1974). In addition, the optimum salinity for each formulation was determined.

The results of the phase behavior study are summarized below.

#### 4.1.1. Rhamnolipid and 1-Butanol (Set RB)

This formulation was made up of a mixture of 1% anionic surfactant rhamnolipid and 3% 1-butanol as a cosolvent. The salinity of the brine was varied from 1% to 20% in 1% increments. This formulation displayed promising results, developing a distinct middle phase microemulsion in all the tubes. The optimum salinity, calculated by the average of all tubes displaying a type III microemulsion, was determined to be 10%.

**Figure 8** shows a phase volume fraction chart for the formulation.

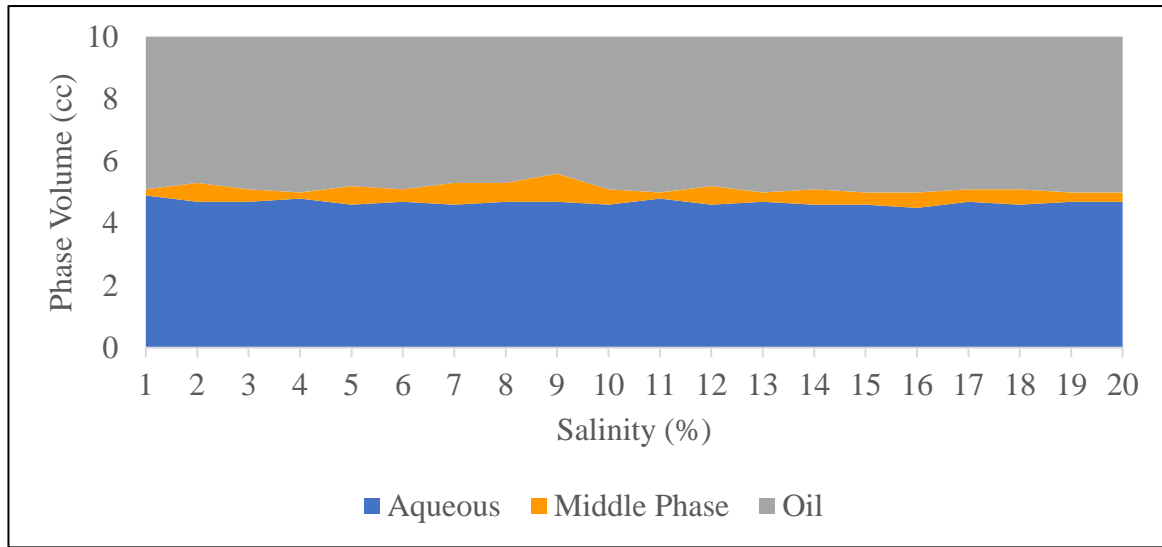


Figure 8 - Results of the phase behavior study (set RB)

#### 4.1.2. Rhamnolipid, APG, and 1-Butanol (Set RAB)

This formulation was made up of a mixture of 1% anionic surfactant rhamnolipid, 1% non-ionic surfactant APG as a co-surfactant and 3% 1-butanol as a cosolvent. The salinity of the brine was varied from 1% to 10% in 1% increments. A distinct middle phase microemulsion was observed in all of the tubes where the salinity was higher than 3%. The optimum salinity was determined to be 7%. **Figure 9** shows a phase volume fraction chart for the formulation.

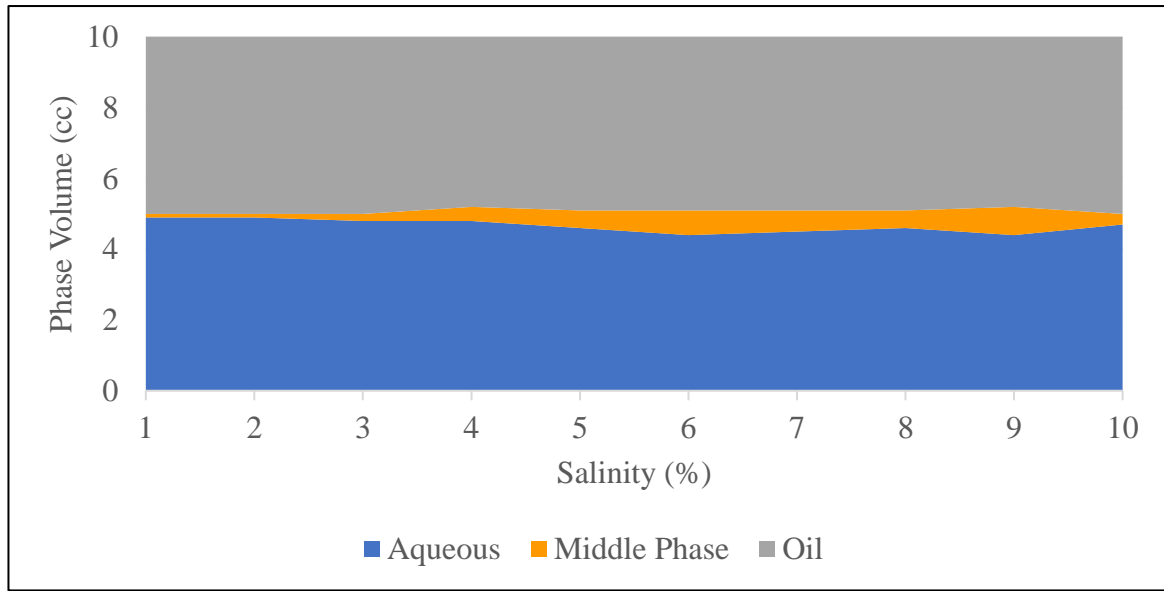


Figure 9 - Results of the phase behavior study (set RAB)

#### 4.1.3. Rhamnolipid and Lecithin (Set LR)

This formulation was made up of a mixture of 2% anionic surfactant rhamnolipid and 2% zwitterionic surfactant lecithin. The salinity of the brine was varied from 1% to 16% in 1% increments. Middle phase microemulsions were observed across all tubes. The optimum salinity was determined to be 5%. **Figure 10** shows a phase volume fraction chart for the formulation.

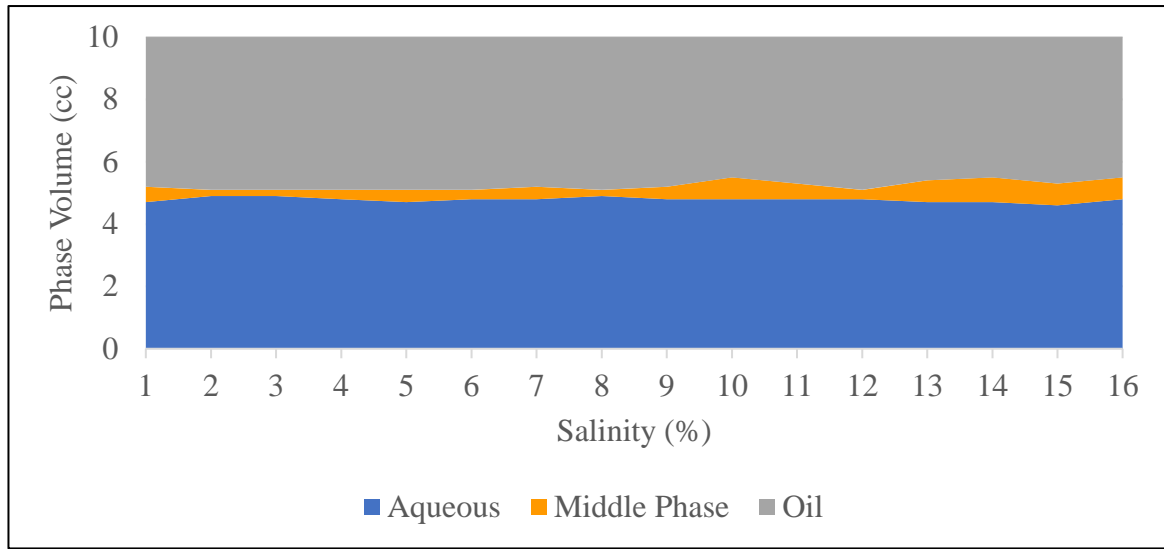


Figure 10 - Results of the phase behavior study (set LRF)

## 4.2. Fluid Properties Tests

### 4.2.1. Viscosity Measurement Results

**Table 8** summarizes the viscosity measurements for the crude oil and brine samples at room and reservoir temperatures. It can be seen that the viscosity of the crude oil was reduced significantly as the temperature increased from 25°C to 52°C. A similar pattern was observed for the brine as well. This trend is expected, because viscosity is strongly and inversely proportional to temperature.

Sample	Viscosity at 25°C (cP)	Viscosity at 52°C (cP)
Crude Oil	19.8	8.2
Brine	1.2	0.7

*Table 8 - Viscosity measurements of the crude oil and brine*

### 4.2.2. Density Measurement Results

Density measurements were conducted for all of the samples in the three sets in addition to oil and the brine samples at both room and reservoir temperatures. **Table 9** lists the density values for each sample. In all of the samples, the density value decreased slightly with the increase of temperature. In addition, because the concentrations used in the formulation sets are very small, the density values for the formulation samples are very close to that of the brine.

Sample Name	Density at 25°C (g/cm <sup>3</sup> )	Density at 52°C (g/cm <sup>3</sup> )
Crude Oil	0.86992	0.84840
Brine	1.01841	1.00135
A1	1.01844	1.00767
A2	1.01837	1.00750
A3	1.01823	1.00697
A4	1.01810	1.00407
A5	1.01638	1.00347
B1	1.01838	1.00487
B2	1.01827	1.00747
B3	1.01819	1.00757
B4	1.01838	1.00766
B5	1.01688	1.00606
C1	1.01860	1.00786
C2	1.01886	1.00813
C3	1.01953	1.00813
C4	1.01904	1.00828
C5	1.01965	1.00887

*Table 9 - Density of the crude oil, brine, and surfactant mixture samples*

#### 4.2.3. Interfacial Tension Measurement

The IFT between the crude oil and brine was measured at ambient temperature and found to be 23 dynes/cm. For the surfactant formulations, the IFT values between the oil and the various samples from the three sets were measured at both room and reservoir temperatures.

##### 4.2.3.1 Set A

**Table 10** outlines the results for the samples in Set A, and the IFT value is plotted against the rhamnolipid concentration in **Figure 11**. The IFT value reaches a minimum of approximately 0.15 dyne/cm at a rhamnolipid concentration of 0.02 wt.%, slightly

increases to approximately 0.2 dyne/cm as the concentration of rhamnolipid increases, then stays at this level. This trend indicates that the CMC, or critical micelle concentration, for this formulation is reached at 0.02 wt.% or less. In addition, it is observed that increasing the temperature from 25°C to 52°C has little effect on the IFT value for all of the measured concentrations.

Sample	Rhamnolipid concentration (wt.%)	1-butanol concentration (wt.%)	IFT at 25°C (dynes/cm)	IFT at 52°C (dynes/cm)
A1	0.02	0.06	0.14407	0.13877
A2	0.04	0.12	0.24657	0.21467
A3	0.06	0.18	0.26126	0.23239
A4	0.08	0.24	0.2324	0.20326
A5	0.5	1.5	0.1842	0.18526

*Table 10 - IFT values of the formulated surfactant samples, set A.*

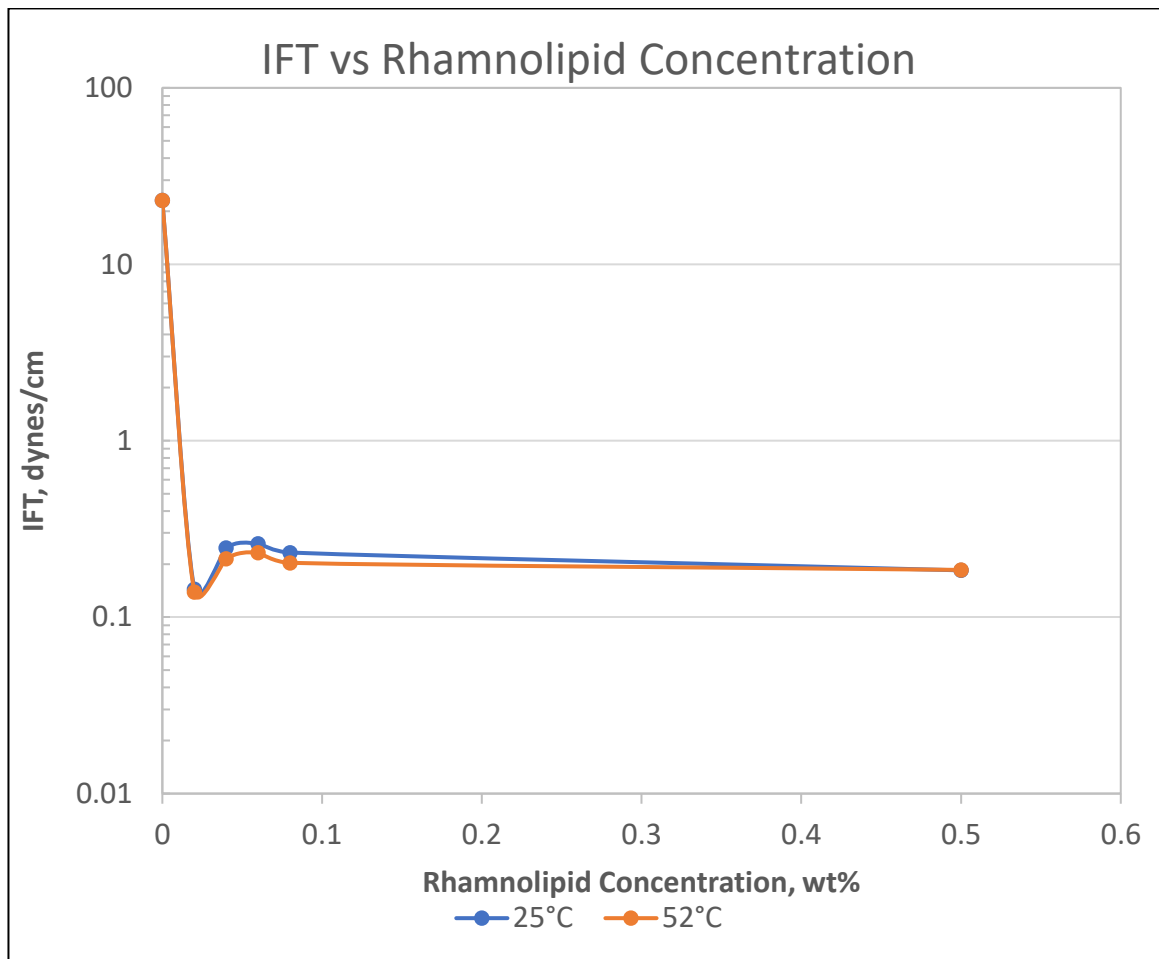


Figure 11 - Plot of the IFT against the rhamnolipid concentration, set A

#### 4.2.3.1 Set B

**Table 11** outlines the results for the samples in Set B, and the IFT value is plotted against rhamnolipid concentration in **Figure 12**. The IFT value reaches a minimum of approximately 0.2 dyne/cm at a rhamnolipid concentration of 0.02 wt.%, and stays at this value as the concentration of rhamnolipid increases. This trend indicates that the CMC for this formulation is 0.02 wt.% or less. In addition, it is observed that increasing the temperature from 25°C to 52°C has little effect on the IFT value for all of the measured concentrations.

Sample	Rhamnolipid Concentration (wt.%)	APG Concentration (wt.%)	1-butanol Concentration (wt.%)	IFT at 25°C (dynes/cm)	IFT at 52°C (dynes/cm)
B1	0.02	0.02	0.06	0.22536	0.23703
B2	0.04	0.04	0.12	0.24097	0.22819
B3	0.06	0.06	0.18	0.23831	0.22394
B4	0.08	0.08	0.24	0.22578	0.20599
B5	0.5	0.5	1.5	0.16887	0.16656

*Table 11 - IFT values of the formulated surfactant samples, set B.*

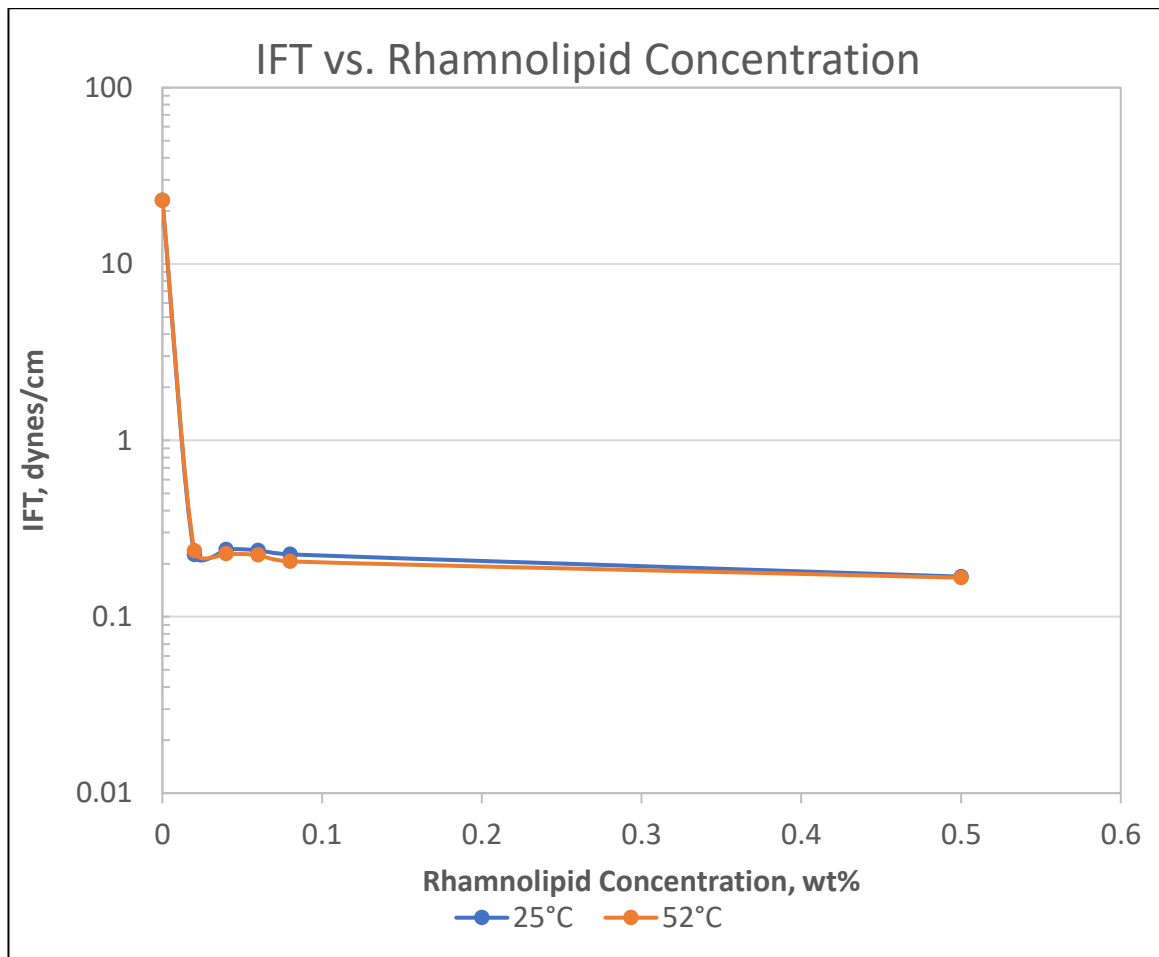


Figure 12 - Plot of the IFT against the rhamnolipid concentration, set B

#### 4.2.3.3 Set C

**Table 12** outlines the results for the samples in Set C, and the IFT value is plotted against rhamnolipid concentration in **Figure 13**. The IFT value reaches a minimum of approximately 0.02 dyne/cm at a rhamnolipid concentration of 0.02 wt.%, slightly increases to approximately 0.5 dyne/cm as the concentration of rhamnolipid increases, then stays at this level. This trend indicates that the CMC for this formulation is 0.04 wt.% or less. In addition, it is observed that increasing the temperature from 25°C to 52°C has little effect on the IFT value at all of the measured concentrations.

Sample	Rhamnolipid Concentration (wt.%)	Lecithin Concentration (wt.%)	IFT at 25°C (dynes/cm)	IFT at 52°C (dynes/cm)
C1	0.02	0.02	0.07535	0.05813
C2	0.04	0.04	0.0189	0.0181
C3	0.06	0.06	0.15116	0.07286
C4	0.08	0.08	0.77669	0.8896
C5	0.25	0.25	0.56347	0.41915

*Table 12 - IFT values of the formulated surfactant samples, set C.*

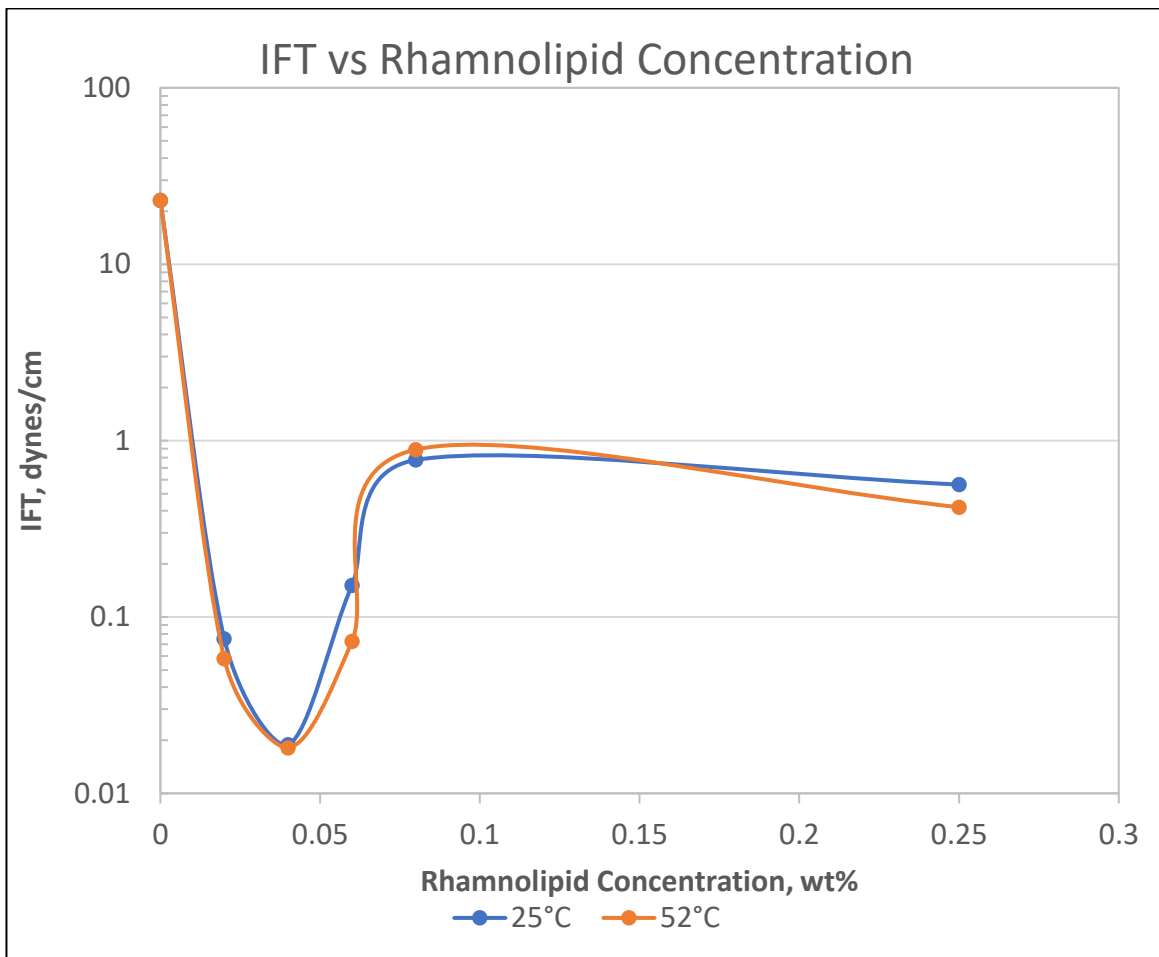


Figure 13 - Plot of the IFT against the rhamnolipid concentration, set C.

### 4.3. Core-Flooding Tests

In this part of the study, three core-flood experiments were conducted to test the EOR capability of three green surfactant mixtures formulations. The first experiment was carried out to investigate the ability of a biosurfactant/alcohol mixture to improve tertiary oil recovery (TOR). The aim of the second experiment was to examine the EOR performance of the previous formulation when the green APG surfactant is added as a co-surfactant for increased stability at high temperatures and salinity levels. The objective of the last core flood experiment was to observe the impact of an alcohol-free green surfactant mixture of rhamnolipid and lecithin on EOR.

In this section, the measured and observed data collected during the three core flooding experiments will be tabulated. In addition, the results will be presented and discussed.

#### 4.3.1. Core Properties

**Table 13** displays the measured core properties for the three sandstone cores used in the core flooding experiments.

Core Sample Number	Length (cm)	Diameter (cm)	Pore Volume (cc)	Dry Weight (g)	Porosity (%)	Permeability (mD)
1	15.2	3.8	34.04	367.41	19.75	176
2	15.1	3.8	36.31	358.77	21.20	145
3	14.9	3.8	35.14	353.34	20.79	132

*Table 13 - Properties of the three Berea sandstone cores used in the core-floods.*

#### 4.3.2. Core Experiment #1

In this experiment, the sandstone core was fully saturated with 3% NaCl brine and then flooded with crude oil until the core reached residual water saturation. The oil-saturated core was then flooded with 3% NaCl brine until it was near residual oil saturation to simulate the water flooding process. The flooding was stopped when only a trace amount of oil was produced or three pore volumes of brine had been injected. The surfactant was a mixture of 0.5% rhamnolipid and 1.5% 1-butanol.

At the end of the oil flood, residual water saturation ( $S_{wr}$ ) was measured at 44.2%. After the water flooding stage was complete, the residual oil saturation ( $S_{or}$ ) was 33.8% and the secondary oil recovery was 39% of the OOIP. The surfactant flooding resulted in an incremental oil recovery of 19.6% and a total oil recovery of 59.1%. Finally, the post flush recovered an additional 3% which brought the total oil recovery to 62.1%. The tertiary oil recovery was 22.6% of the OOIP. **Table 14** details the amount recovered and fluid saturations during the different stages, and **Figure 14** shows the total oil recovery versus the total injected pore volume during the brine flooding, surfactant flooding, and post flush.

Stage	PV <sub>w</sub> (cc)	S <sub>w</sub> (%)	PV <sub>o</sub> (cc)	P <sub>o</sub> (cc)	S <sub>o</sub> (%)	Oil Recovery (%)	Incremental Oil Recovery (%)
Initial	34.04	100.0%	0.00		0.0%		
Oil Flooding	15.04	44.2%	19.00	0.00	55.8%		
Brine Flooding	22.53	66.2%	11.51	7.49	33.8%	39.4%	39.4%
Surfactant Flooding	26.26	77.1%	7.78	3.73	22.9%	59.1%	19.6%
Post-Flush	26.83	78.8%	7.21	0.57	21.2%	62.1%	3.0%

Table 14 - Measured and observed data for the core flooding experiment (Core #1)

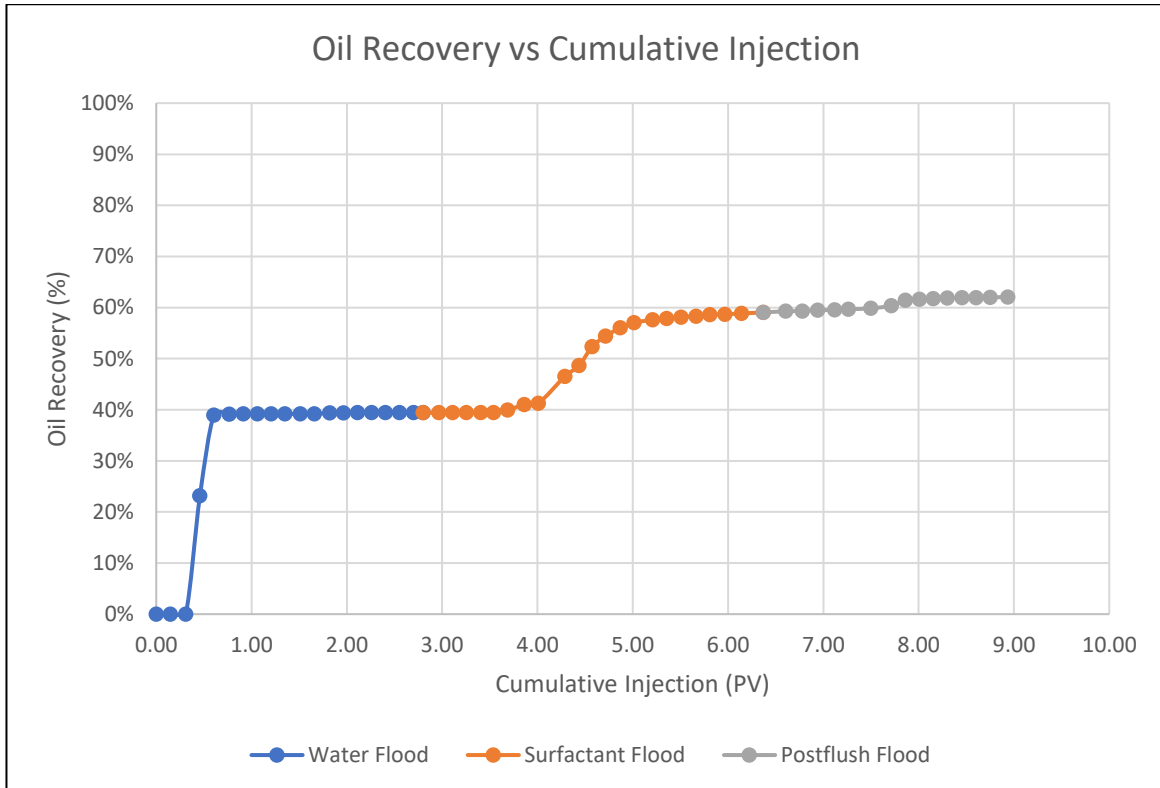


Figure 14 - Oil recovery vs. cumulative injection (Core #1)

#### 4.3.3. Core Experiment #2

In this experiment, the sandstone core was fully saturated with 3% NaCl brine and then flooded with crude oil until the core reached residual water saturation. The oil saturated core was then flooded with 3% NaCl brine until it was near residual oil saturation to simulate the water flooding process. The flooding was stopped when only a trace amount of oil was produced or three pore volumes of brine had been injected. The surfactant was a mixture of 0.5% rhamnolipid, 0.5% APG, and 1.5% 1-butanol.

At the end of the oil flood, residual water saturation ( $S_{wr}$ ) was measured at 42.2%. After the water flooding stage was complete, the residual oil saturation ( $S_{or}$ ) was 31.5% and the secondary oil recovery was 45.5% of the OOIP. The surfactant flooding resulted in a modest incremental oil recovery of 3.4 % and a total oil recovery of 48.9 %. Finally, the post flush recovered an additional 6.4%, bringing the total oil recovery to 55.3%. The tertiary oil recovery was 9.8% of the OOIP. **Table 15** details the amount recovered and fluid saturations during the different stages, and **Figure 15** shows the total oil recovery versus the total injected pore volume during the brine flooding, surfactant flooding, and post flush.

Stage	PV <sub>w</sub> (cc)	S <sub>w</sub> (%)	PV <sub>o</sub> (cc)	P <sub>o</sub> (cc)	S <sub>o</sub> (%)	Oil Recovery (%)	Incremental Oil Recovery (%)
Initial	36.31	100.0%	0.00		0.0%		
Oil Flooding	15.31	42.2%	21.00	0.00	57.8%		
Brine Flooding	24.86	68.5%	11.45	9.55	31.5%	45.5%	45.5%
Surfactant Flooding	25.57	70.4%	10.74	0.71	29.6%	48.9%	3.4%
Post-Flush	26.92	74.1%	9.39	1.35	25.9%	55.3%	6.4%

Table 15 - Measured and observed data for the core flooding experiment (Core #2)

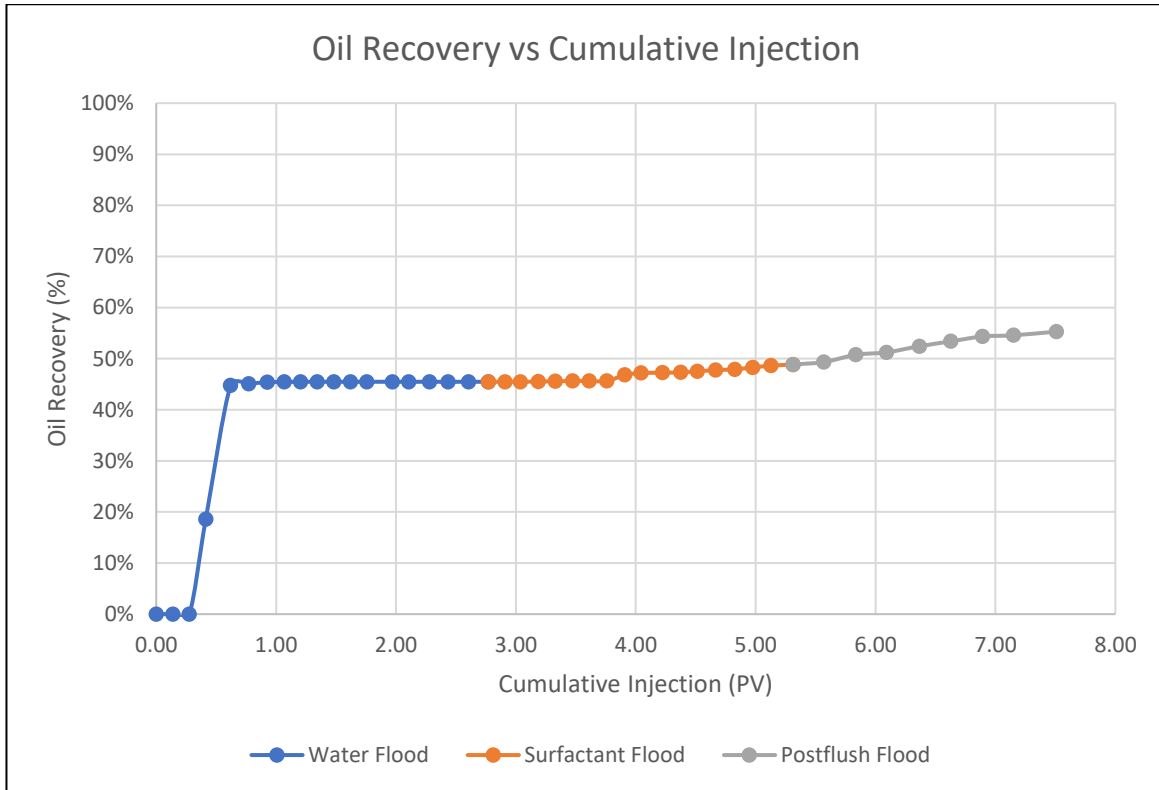


Figure 15 - Oil recovery vs. cumulative injection (Core #2)

#### 4.3.4. Core Experiment #3

In this experiment, the sandstone core was fully saturated with 3% NaCl brine and then flooded with crude oil until the core reached residual water saturation. The oil saturated core was then flooded with 3% NaCl brine until it was near residual oil saturation to simulate the water flooding process. The flooding was stopped when only a trace amount of oil was produced or three pore volumes of brine had been injected. The surfactant was a mixture of 0.25% rhamnolipid and 0.25 % lecithin.

At the end of the oil flood, residual water saturation ( $S_{wr}$ ) was measured at 43.1%. After the water flooding stage was complete, the residual oil saturation ( $S_{or}$ ) was 31.0% and the secondary oil recovery was 46% of the OOIP. The surfactant flooding resulted in an incremental oil recovery of 14.3% and a total oil recovery of 59.9%. Finally, the post flush recovered an additional 9.8%, bringing the total oil recovery to 69.6%. The tertiary oil recovery was 24% of the OOIP. **Table 16** details the amount recovered and fluid saturations during the different stages, and **Figure 16** shows the total oil recovery versus the total injected pore volume during the brine flooding, surfactant flooding, and post flush.

Stage	PV <sub>w</sub> (cc)	S <sub>w</sub> (%)	PV <sub>o</sub> (cc)	P <sub>o</sub> (cc)	S <sub>o</sub> (%)	Oil Recovery (%)	Incremental Oil Recovery (%)
Initial	35.14	100.0%	0.00		0.0%		
Oil Flooding	15.14	43.1%	20.00	0.00	56.9%		
Brine Flooding	24.26	69.0%	10.88	9.12	31.0%	45.6%	45.6%
Surfactant Flooding	27.11	77.1%	8.03	2.85	22.9%	59.9%	14.3%
Post-Flush	29.06	82.7%	6.08	1.95	17.3%	69.6%	9.8%

Table 16 - Measured and observed data for the core flooding experiment (Core #3)

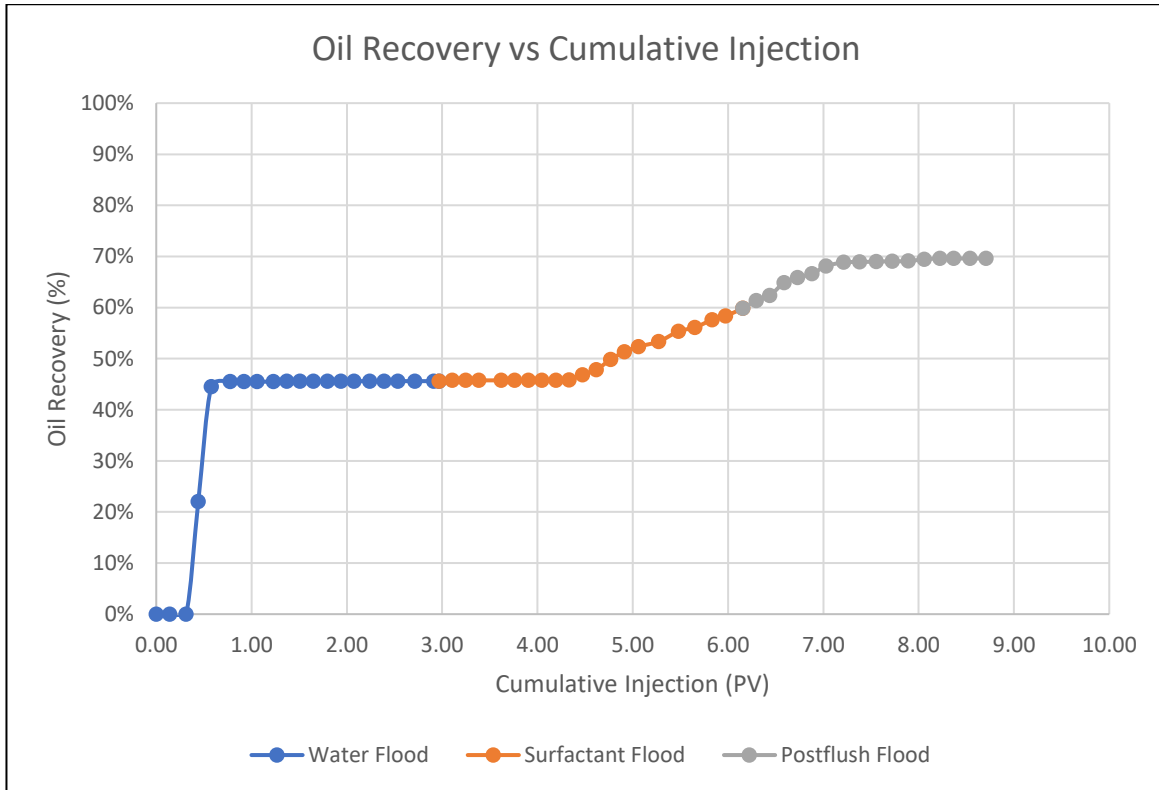


Figure 16 - Oil recovery vs. cumulative injection (Core #3)

#### 4.3.5 Comparison of the Three Formulations

A summary of the three formulation results is shown in **Table 17**. The oil recovery at the different stages, secondary and tertiary, for the three cases is illustrated in **Figure 17**. The rhamnolipid/lecithin formulation performed best, with a TOR of 24%. The rhamnolipid/butanol formulation achieved a similar, albeit slightly smaller, value of 22.6% for the TOR. The rhamnolipid/APG/butanol mixture resulted in a significantly smaller TOR value of 9.8%.

Exp. No	Core No.	Formulation	Secondary Oil Recovery %	Tertiary Oil Recovery %	Total Oil Recovery %
1	1	0.5 % Rhamnolipid 1.5 % Butanol	39.4	22.6	62.1
2	2	0.5 % Rhamnolipid 0.5 % APG 1.5 % Butanol	45.5	9.8	55.3
3	3	0.25 % Rhamnolipid 0.25 % Lecithin	45.6	24	69.6

*Table 17 - Summary of the EOR results for the three formulations.*

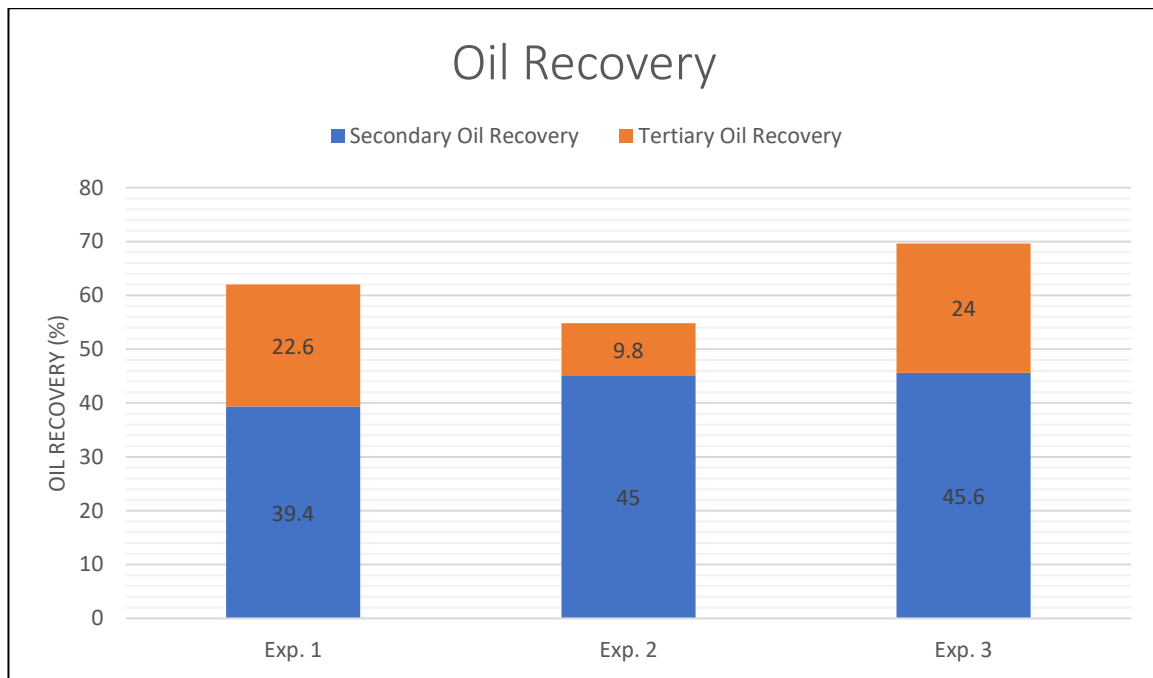


Figure 17 – Comparison of the oil recovery for the developed formulations

## 4.4. Simulation of Core-Flooding Experiment

Core floods using three green surfactant formulations was simulated and the results were compared with laboratory core flooding data to verify the simulation accuracy. The anionic surfactant rhamnolipid combined with 1-butanol as a co-solvent were simulated first. The second experiment simulated the second formulation, which was made up of the anionic surfactant rhamnolipid as the primary surfactant, the green surfactant APG as a co-surfactant, and 1-butanol as the co-solvent. Finally, a formulation containing the anionic surfactant rhamnolipid as the primary surfactant and the zwitterionic surfactant lecithin as co-surfactant was simulated. In all cases, secondary and tertiary recoveries of the oil were recorded. The following sections present the simulation results.

### 4.4.1 Formulation 1: Rhamnolipid and 1-Butanol

Water injection commenced through the injection well at a rate of 30 cc/hour until about three pore volumes of water had been injected, to simulate the water flooding process. Oil recovery due to the water injection was 37% of OOIP, which is very close to the value obtained during the core flooding experiment, 39%.

After the conclusion of the water injection phase, the surfactant was introduced into the injected water in the injection well and the injection was resumed at the same rate until another three pore volumes of water had been injected, to simulate the surfactant

flooding process. The total oil recovery increased to 62% after the surfactant flood, slightly higher than the 59% recovery obtained during the core flooding experiment.

To simulate the post-flush process, injection of the surfactant was stopped, and the injection of water was continued at the same rate until about three more pore volumes of water had been injected. In the simulation, oil recovery increased slightly, reaching 63% of the OOIP, while in the core flooding experiment the post-flush increased the oil recovery to 62%.

The oil recovery during the various stages of flooding in both the simulation and the core flooding experiment is illustrated in **Figure 18**. Overall, the oil recovery from the simulation matches closely to the recovery observed in the core experiments. The simulation oil recovery curve is smoother because the oil recovery amount can be generated frequently—for example, after each time step—during the simulation run, while in the core flooding experiment the oil recovery can be calculated only after at least 5 mL of fluid has been collected in the collection tube. The mismatch seen in the initial part of the plot can be attributed to the fact that the first 11 mL of oil produced during the core flooding experiment was discarded because it was produced from the dead volume of oil in the equipment tubes. During the simulation, on the other hand, oil production started shortly after the water injection without the delay of draining dead oil from the equipment.

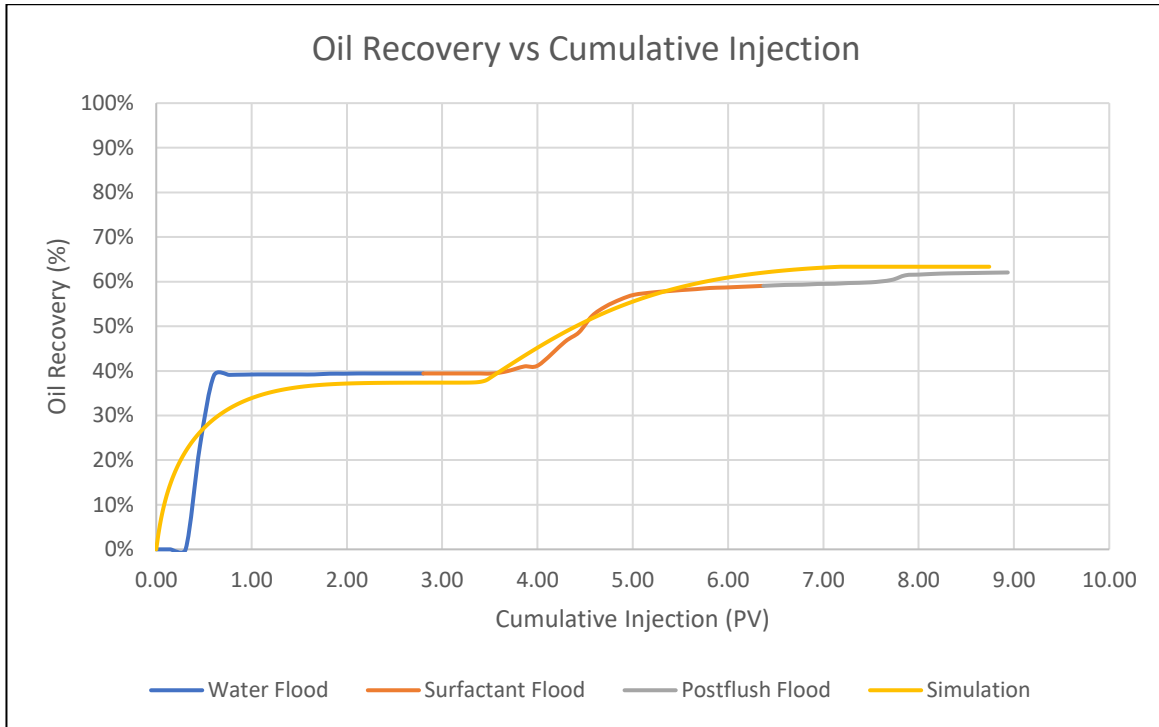


*Figure 18 - Total oil recovery observed during core flooding and simulation for the first formulation*

#### 4.4.2 Formulation 2: Rhamnolipid, APG, and 1-Butanol

Water injection commenced through the injection well at a rate of 30 cc/hour until about three pore volumes of water had been injected, to simulate the water flooding process. Oil recovery due to the water injection was 43% of OOIP, which is very close to the value obtained during the core flooding experiment, 45%.

After the conclusion of the water injection phase, the surfactant was introduced into the injected water in the injection well and the injection was resumed at the same rate until another three pore volumes of water had been injected, to simulate the surfactant flooding process. The total oil recovery increased to 53% after the surfactant flood, slightly higher than the 49% recovery obtained during the core flooding experiment.

To simulate the post-flush process, injection of the surfactant was stopped, and the injection of water was continued at the same rate until about three more pore volumes of water had been injected. In the simulation, oil recovery increased slightly, reaching 55% of the OOIP, which was nearly identical to that of the core flooding experiment.

The oil recovery during the various stages of flooding in both the simulation and the core flooding experiment is illustrated in **Figure 19**. Overall, the oil recovery from the simulation matches closely to the recovery observed in the core experiments. The simulation oil recovery curve is smoother because the oil recovery amount can be generated frequently—for example, after each time step—during the simulation run, while in the core flooding experiment the oil recovery can be calculated only after at least 5 mL of fluid has been collected in the collection tube. The mismatch seen in the initial part of the plot can be attributed to the fact that the first 11 mL of oil produced during the core

flooding experiment was discarded because it was produced from the dead volume of oil in the equipment tubes. During the simulation, on the other hand, oil production started shortly after the water injection without the delay of draining dead oil from the equipment.

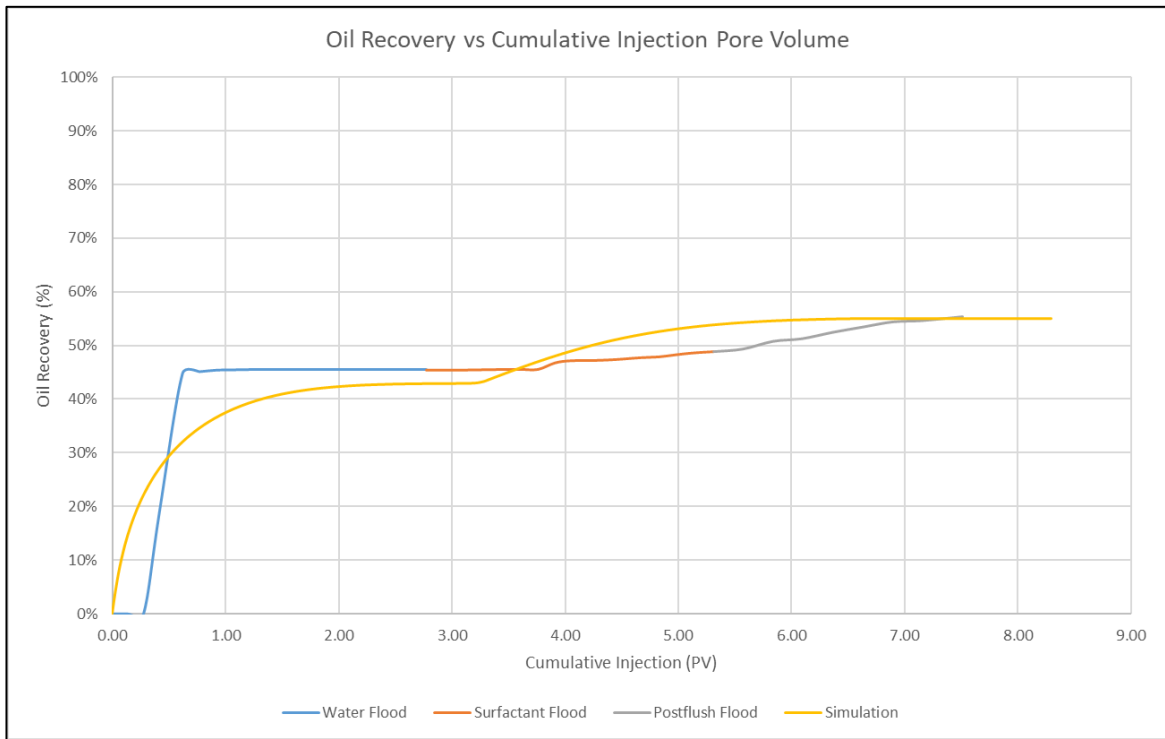


Figure 19 - Total oil recovery observed during core flooding and simulation for the second formulation

#### 4.4.3 Formulation 3: Rhamnolipid and Lecithin

Water injection commenced through the injection well at a rate of 30 cc/hour until about three pore volumes of water had been injected, to simulate the water flooding process. Oil recovery due to the water injection was 43% of OOIP, which is very close to the value obtained during the core flooding experiment, 46%.

After the conclusion of the water injection phase, the surfactant was introduced into the injected water in the injection well and the injection was resumed at the same rate until another three pore volumes of water had been injected, to simulate the surfactant flooding process. The total oil recovery increased to 64% after the surfactant flood, slightly higher than the 60% recovery obtained during the core flooding experiment.

To simulate the post-flush process, injection of the surfactant was stopped, and the injection of water was continued at the same rate until about three more pore volumes of water had been injected. In the simulation, oil recovery increased slightly, reaching 67% of the OOIP, while in the core flooding experiment the post-flush increased the oil recovery to nearly 70%.

The oil recovery during the various stages of flooding in both the simulation and the core flooding experiment is illustrated in **Figure 20**. Overall, the oil recovery from the simulation matches closely to the recovery observed in the core experiments. The simulation oil recovery curve is smoother because the oil recovery amount can be generated frequently—for example, after each time step—during the simulation run, while in the core flooding experiment the oil recovery can be calculated only after at least 5 mL of fluid has been collected in the collection tube. The mismatch seen in the initial part of

the plot can be attributed to the fact that the first 11 mL of oil produced during the core flooding experiment was discarded because it was produced from the dead volume of oil in the equipment tubes. During the simulation, on the other hand, oil production started shortly after the water injection without the delay of draining dead oil from the equipment.

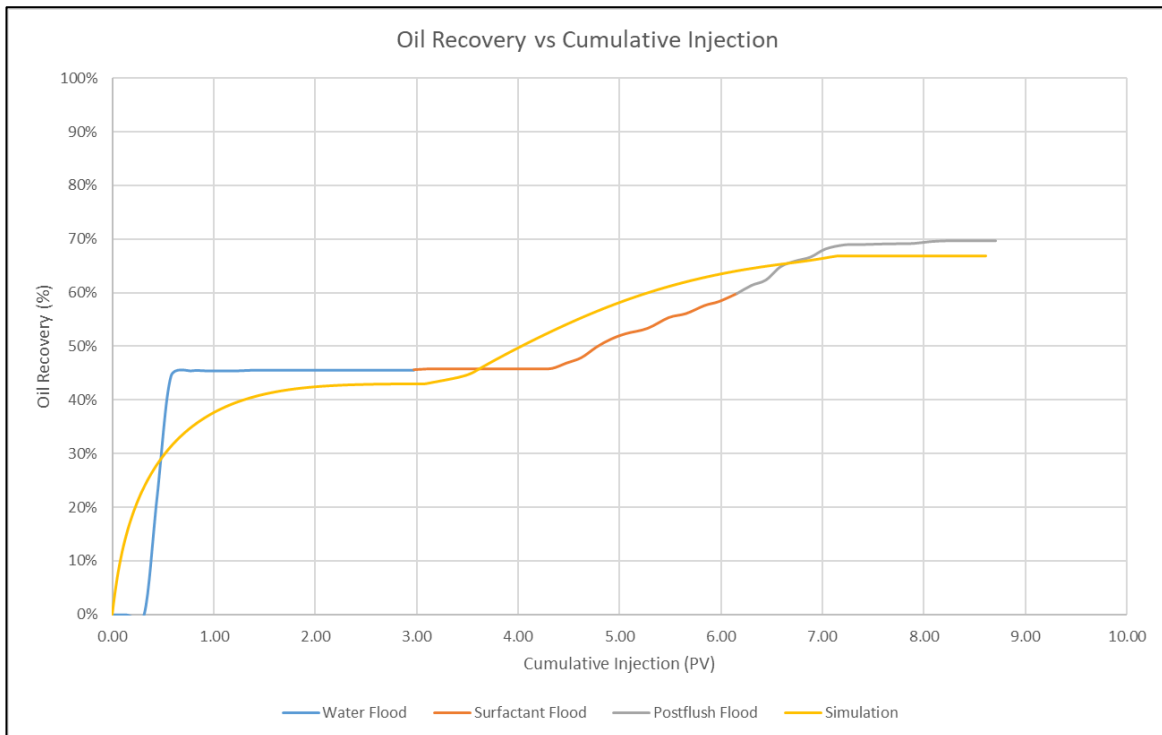


*Figure 20 - Total oil recovery observed during core flooding and simulation for the third formulation*

## 4.5 Conclusions

1. Overall, it is concluded that two of the surfactant formulations tested in this study performed strongly in all of the performed tests and have potential for use in enhanced oil recovery processes.
2. A surfactant formulation consisting of 1% anionic surfactant rhamnolipid and 3% butanol gives a stable middle phase microemulsion when the salinity is within the range of 1%-20%. In addition, blending the previous formulation with 1% APG shows a stable middle phase microemulsion over a salinity range of 3%-9%. Finally, a formulation of 2% anionic surfactant rhamnolipid and 2% zwitterionic surfactant lecithin generates a stable middle phase microemulsion over a salinity range of 1%-10%.
3. The rhamnolipid/lecithin surfactant formulation reduces the interfacial tension between the crude oil and the brine to a low value of  $10^{-2}$  dynes/cm. On the other hand, the formulations that consist of rhamnolipid/butanol or rhamnolipid/APG/butanol lower the interfacial tension between the crude oil and the brine to 0.2 dyne/cm.
4. Temperature was found to have a negligible impact on the value of the measured IFT in all three of the tested formulations.
5. The rhamnolipid/butanol and rhamnolipid/lecithin surfactants formulations have been successful in recovering additional amounts of oil after the waterflooding process. During the core flooding experiments, the first formulation recovered 22.6% of the OOIP while the second recovered 24% of the OOIP.
6. The rhamnolipid/APG/butanol formulation was not successful at recovering any significant amount of oil during the core flooding test.
7. Secondary and tertiary oil recoveries due to water and surfactant flooding in core flooding experiments can be accurately modeled using Eclipse simulator. For each of the three formulations,

the oil recovery plot generated by the simulation matched closely with the one obtained during the core flooding procedure.

8. In the core-flooding experiment for the first formulation (RB), the tertiary recovery was 22.6% of the OOIP, and the total oil recovery was 62.1%. The simulation showed results of 26% and 63% for the tertiary and total oil recoveries, respectively. This shows a good match between the experimental results and the simulation.

9. In the core-flooding experiment for the second formulation (RAB), the tertiary recovery was 9.8% of the OOIP, and the total oil recovery was 55.3%. The simulation showed results of 12% and 55% for the tertiary and total oil recoveries, respectively. This shows a good match between the experimental results and the simulation.

10. In the core-flooding experiment for the third formulation (RL), the tertiary recovery was 24% of the OOIP, and the total oil recovery was 69.6%. The simulation showed results of 24% and 67% for the tertiary and total oil recoveries, respectively. This shows a good match between the experimental results and the simulation.

## 4.6 Recommendations

The following are recommendations for additional work:

1. It is recommended that a real reservoir brine is used in place of the NaCl solution in order to more accurately simulate the conditions at the reservoir.
2. It is recommended that the parameters of a real reservoir here in Saudi Arabia be used to test the developed formulations, such as the temperature and/or pressure found in one specific reservoir.
3. It is recommended that the formulations be tested for efficacy in other types of reservoirs, such as carbonate reservoirs.
4. It is recommended that surfactant adsorption studies be conducted to determine the adsorption parameters for the surfactants used.
5. It is recommended to utilize the developed simulation models to perform sensitivity analyses to investigate the effect of different parameters on the performance of surfactants in core flooding experiments.

## APPENDIX A

### A.1. Rhamnolipid Literature Survey Summary

Author	Title	Study Type	Results
<b>Xiangdong et. al (2007)</b>	Engineering Bacteria for Production of Rhamnolipid as an Agent for Enhanced Oil Recovery	IFT measurement Sand pack flood	Reduced IFT from 35 dynes/cm to 0.3 dynes/cm between water and n-octane  40% residual oil recovery was obtained from sand pack flooding
<b>Amani (2015a)</b>	Study of enhanced oil recovery by Rhamnolipids in a homogeneous 2D micromodel	IFT measurement Fluid properties experiment Simulated chemical flooding	Found to remain effective from pH levels between 4 and 10, temperatures as high as 100° C, and salinity concentrations up to 25g/L  Reduced surface tension of water from 72 dynes/cm to 25 dynes/cm, and IFT between prepared surfactant and 34° API crude oil to 2 dynes/cm  5% OOIP recovered from the surfactant flood in the micromodel
<b>Amani (2015b)</b>	Evaluation of Biosurfactants and Surfactants for Crude Oil Contaminated Sand Washing	IFT measurement Emulsification index Sand pack flood	The Rhamnolipid achieved the highest emulsification level of 88%, compared with the other three tested surfactants  At both room temperature (25° C) and at 50°C, the Rhamnolipid outperformed the other surfactants, recovering 80% at room temperature and 90% at 50° C of the residual oil in the contaminated sand
<b>Khaleel (2017)</b>	Selecting an Optimal Surfactant for Use in EOR: An Experimental Study	Salinity scan IFT measurement Wettability study	Formed a middle phase micro emulsion at 80K and 90K ppm salinities  Reduced IFT to 0.5 dynes/cm  Changed oil-wet carbonate core to slightly less oil-wet.
<b>Gudina et. al (2015)</b>	Bioconversion of agro-industrial by-products in Rhamnolipids toward applications in enhanced oil	Sand pack flood	The Rhamnolipid recovered 55% of the oil in the sand pack, performing better than synthetic commercial surfactants

	recovery and bioremediation		
<b>Rocha et. al (1992)</b>	Biosurfactant production by two isolates of <i>Pseudomonas aeruginosa</i>	Fluid properties experiment CMC determination	The Rhamnolipid produced stable emulsions of heavy and extra-heavy crude oils at temperatures as low as 0° C and as high as 100° C.  The biosurfactant was able to reduce the surface tension of water from 72 to 28 dynes/cm.
<b>Shafeeq et. al (1989)</b>	Degradation of different hydrocarbons and production of biosurfactant by <i>Pseudomonas aeruginosa</i> isolated from coastal waters	Surface tension Emulsification index	While no numbers were reported, it is mentioned that due to the emulsification properties of the Rhamnolipid, it was found to be very effective at dispersing oil in oil spill clean-up tests

Table 18 - Literature Survey Summary, Rhamnolipid

## A.2. APG Literature Survey Summary

Author	Title	Study Type	Results
<b>Iglauer et. al (2009)</b>	Alkyl polyglycoside surfactant-alcohol cosolvent formulations for improved oil recovery	Phase behavior IFT measurement Fluid properties experiment Core flood	Ultra-low IFT could be created with certain APG-alcohol formulations, reaching as low as 0.001 mN/m.  Roughly 85% of the OOIP was recovered in the core-flood experiments. The tertiary recovery was over 50% of the residual oil within the core
<b>Iglauer et. al (2010)</b>	New surfactant classes for enhanced oil recovery and their tertiary oil recovery potential	Core flood Sand pack flood IFT measurement	Their APG formulations recovered 40.8% and 53% of tertiary oil recovery respectively, with the sand pack flood formulation recovering 94% of the original oil in place (OOIP).
<b>Ghosh and Obassi (2013)</b>	Eco-Friendly Surfactant for EOR in High Temperature, High Salinity Carbonate Reservoir	Phase behavior Salinity screening Fluid properties experiment Spontaneous imbibition	One of the APG surfactants performed effectively even at the highest levels of temperature and salinity in the experiment, and so it was concluded that it is a viable surfactant for use in carbonate reservoir EOR techniques
<b>Yin and Zhang (2013)</b>	Evaluation and research on performance of a blend surfactant system of alkyl	IFT measurement Wettability tests Core flood	The APG surfactant was able to reduce the IFT to 0.00216 mN/m at a concentration of 0.5% by weight

	polyglycoside in carbonate reservoir		<p>It was also able to change the rock surface from oil-wet to water-wet in the wettability tests.</p> <p>It was found that the surfactant was able to remain stable at high levels of both salinity and temperature.</p>
<b>Santa et. al (2011)</b>	Sustainable Surfactants in Enhanced Oil Recovery	Phase behavior IFT measurement Salinity scan	<p>The authors found that short-chain and mid-chain APG surfactants performed best under extreme conditions compared to other APG surfactant types</p> <p>They also found that stable microemulsions could be formed when the APG surfactants are combined with a co-solvent</p>

*Table 19 - Literature Survey Summary, APG*

## APPENDIX B

### B.1. Simulation Input Data for Formulation RB

$S_w$	$K_{rw}$	$K_{ro}$	$S_o$
0.44	0	1	0.56
0.66	1	0	0.338

*Table 20 - Relative permeability and saturation data for formulation #1 (RB)*

Property Type	Value
Oil Density (g/cm <sup>3</sup> )	0.8484
Water Density (g/cm <sup>3</sup> )	1.00135
Oil Viscosity (cP)	8.2
Water Viscosity (cP)	1.2
Adsorption Function	0.0002
Initial IFT (dynes/cm)	23
Final IFT (dynes/cm)	0.2
Liquid Rate (cc/min)	0.5

*Table 21 - Fluid property data for formulation #1 (RB)*

### B.2. Simulation Input Data for Formulation RAB

$S_w$	$K_{rw}$	$K_{ro}$	$S_o$
0.422	0	1	0.578
0.685	1	0	0.315

*Table 22 - Relative permeability and saturation data for formulation #2 (RAB)*

Property Type	Value
Oil Density (g/cm <sup>3</sup> )	0.8484
Water Density (g/cm <sup>3</sup> )	1.00135
Oil Viscosity (cP)	8.2
Water Viscosity (cP)	1.2
Adsorption Function	0.0002
Initial IFT (dynes/cm)	23
Final IFT (dynes/cm)	0.2
Liquid Rate (cc/min)	0.5

*Table 23 - Fluid property data for formulation #2 (RAB)*

### B.3. Simulation Input Data for Formulation RL

$S_w$	$K_{rw}$	$K_{ro}$	$S_o$
0.43	0	1	0.57
0.69	1	0	0.31

Table 24 - Relative permeability and saturation data for formulation #3 (RL)

Property Type	Value
Oil Density (g/cm <sup>3</sup> )	0.8484
Water Density (g/cm <sup>3</sup> )	1.00135
Oil Viscosity (cP)	8.2
Water Viscosity (cP)	1.2
Adsorption Function	0.0002
Initial IFT (dynes/cm)	23
Final IFT (dynes/cm)	0.41
Liquid Rate (cc/min)	0.5

Table 25 - Fluid property data for formulation #3 (RL)

## REFERENCES

- Abd-Allah, A. (1995). Determination of long chain alkylbenzenes in sediment samples from Alexandria Coast, Egypt. *Toxicological and Environmental Chemistry*, 47, 83-88.
- Abel, P. (1974). Toxicity of Synthetic Detergents to Fish and Aquatic Invertebrates. *Journal of Fish Biology*, 6, 279-298.
- Abel, P. (1976). Toxic Action of Several Lethal Concentrations of an Anionic Detergent on the Gills of the Brown Trout. *Journal of Fish Biology*, 9, 441-446.
- Ahmed, T. (2007). *Equations of State and PVT Analysis: Applications for Improved Reservoir Modeling*. Houston, TX: Gulf Professional Publishing.
- Amani, H. (2015, March 16). Evaluation of Biosurfactants and Surfactants for Crude Oil Contaminated Sand Washing. *Petroleum Science and Technology*, 33(5), 510-519.  
doi:10.1080/10916466.2014.999941
- Amani, H. (2015). Study of enhanced oil recovery by rhamnolipids in a homogeneous 2D micromodel. *Journal of Petroleum Science and Engineering*, 128, 212-219.
- Banat, I. (1995). Biosurfactants Production and Possible Uses in Microbial Enhanced Oil Recovery and Oil Pollution Remediation: A Review. *Bioresource Technology*, 51, 1-12.
- Banat, I. M. (1993, June). The isolation of a thermophilic biosurfactant producing *Bacillus* SP. *Biotechnology Letters*, 15(6), 591-594.

- Barbieri, E., Ngan, P., & Gomez, V. (1998). The effect of SDS, sodium dodecyl sulfate, on the metabolism and swimming capacity of Cyprinus carpio. *Revista Brasileira de Biologia*, 58, 263-271.
- Bardach, J., Fujiya, M., & Holl, A. (1965). Detergents: Effects on the Chemical Senses of the Fish Ictalurus Natalis (le Sueur). *Science*, 148, 1605-1607.
- Bourrel, M., Salager, J., Schechter, R., & Wade, W. (1980). A correlation for phase behavior of nonionic surfactants. *Journal of Colloid and Interface Science*, 75(2), 451-461. doi:[https://doi.org/10.1016/0021-9797\(80\)90470-1](https://doi.org/10.1016/0021-9797(80)90470-1)
- Boyd, J., Parkinson, C., & Sherman, P. (1972, November). Factors Affecting Emulsion Stability, and the HLB Concept. *Journal of Colloid and Interface Science*, 41(2).
- Cash, L., Cayias, J. L., Fournier, G., Macallister, D., Schares, T., Schechter, R. S., & Wade, W. H. (1977). The application of low interfacial tension scaling rules to binary hydrocarbon mixtures. *Journal of Colloid and Interface Science*, 39-44.
- Cayias, J., Schechter, R., & Wade, W. (1976). Modeling crude oils for low interfacial tension. *Society of Petroleum Engineers Journal*, 351-357.
- Davies, J. (1957). A Quantitative Kinetic Theory of Emulsion Type. I. Physical Chemistry of the Emulsifying Agent. *2nd International Congress Surface Activity*. 426, p. 13. London: Butterworths Scientific Publication.
- Desai, J., & Banat, I. (1997). Microbial Production of Surfactants and Their Commercial Potential. *Microbiology and Molecular Biology Reviews*, 61, 47-64.

Dubeau, D., Deziel, E., Woods, D. E., & Lepine, F. (2009). *Burkholderia thailandensis* harbors two identical rhl gene clusters responsible for the biosynthesis of rhamnolipids. *BMC Microbiology*, 9, 263.

Fava, F., & Gioia, D. (2001). Soya lecithin effects on the aerobic biodegradation of polychlorinated biphenyls in an artificially contaminated soil. *Biotechnology and Bioengineering*, 72(2), 177-184.

Georgiou, G., Lin, S., & Sharma, M. (1992). Surface-Active Compounds from Microorganisms. *Biotechnology*, 10, 60-65.

Ghosh, B., & Obassi, D. (2013). Eco-Friendly Surfactant for EOR in High Temperature, High Salinity Carbonate Reservoir. *Society of Petroleum Engineers*. Kuala Lumpur: SPE International.

Green, D. W., & Wilhite, G. P. (1997). *Enhanced Oil Recovery*. Society of Petroleum Engineers.

Griffin, W. C. (1949). Classification of Surface-Active Agents by HLB., (p. 16). Chicago.

Griffin, W. C. (1954). Calculation of HLB Values of Non-Ionic Surfactants., (p. 8). New York.

Gudina, E. J., Rodrigues, A. I., Alves, E., Domingues, M. R., Teixeira, J. A., & Rodrigues, L. R. (2015). Bioconversion of agro-industrial by-products in rhamnolipids toward applications in enhanced oil recovery and bioremediation. *Bioresource Technology*(177), 87-93.

Gunther IV, N. W., Nunez, A., Fett, W., & Solaiman, D. K. (2005, May). Production of Rhamnolipids by *Pseudomonas chloraphis*, a Nonpathogenic Bacterium. *Applied and Environmental Microbiology*, 71(5), 2288-2293.

doi:10.1128/AEM.71.5.2288-2293.2005

Haq, M. B. (2012). *The Role of Green Surfactants in Microbial Enhanced Oil Recovery*. The University of Western Australia, School of Mechanical and Chemical Engineering. The University of Western Australia.

Healy, R. N., & Reed, R. L. (1974). Physsicochemical Aspects of Microemulsion Flooding. *Society of Petroleum Engineers Journal*, 491-501.

Healy, R. N., Reed, R. L., & Stenmark, D. G. (1976). Multiphase microemulsion systems. *Society of Petroleum Engineers Journal*, 147-160.

Hill, K., von Rybinski, W., & Stoll, G. (1997). *Alkyl Polyglycosides*. Weinheim, Germany: VCH Verlagsgesellschaft mbH.

Iglauer, S., Wu, Y., Shuler, P., Tang, Y., & Goddard III, W. A. (2009). Alkyl polyglycoside surfactant-alcohol cosolvent formulations for improved oil recovery. *Colloids and Surfaces A: Physicochemical and Engineering Aspects*, 339, 48-59.

Iglauer, S., Wu, Y., Shuler, P., Tang, Y., & Goddard III, W. A. (2010). New surfactant classes for enhanced oil recovery and their tertiary oil recovery potential. *Journal of Petroleum Science and Engineering*, 71, 23-29.

Khaleel, O. T. (2017). *Selecting an Optimal Surfactant for Use in EOR: An Experimental Study*. Colorado School of Mines, Petroleum Engineering. Ann Arbor: ProQuest LLC.

Kloet, J. V., & Schramm, L. L. (2002, January). The Effect of Shear and Oil/Water Ratio on the Required Hydrophile-Lipophile Balance for Emulsification. *Journal of Surfactants and Detergents*, 5(1), 19-24.

Kronberg, B., Holmberg, K., & Lindman, B. (2014). *Surface Chemistry of Surfactants and Polymers*. West Sussex, United Kingdom: John Wiley & Sons.

KRÜSS. (2015). Spinning Drop Tensiometer - SITE100 / SITE100HS User Manual. Hamburg, Germany: KRÜSS GmbH.

Lewis, M. (1991). Chronic and Sublethal Toxicities of Surfactants to Aquatic Animals: A Review and Risk Assessment. *Water Research*, 25, 101-113.

Lichtfouse, E., Schwarzbauer, J., & Robert, D. (2013). *Pollutant Diseases, Remediation, and Recycling*. Switzerland: Springer International Publishing.

Liwarska-Bizukojc, E., Miksch, K., Malachowska-Jutsz, A., & Kalka, J. (2005). Acute Toxicity and Genotoxicity of Five Selected Anionic and Nonionic Surfactants. *Chemosphere*, 58, 1249-1253.

Mallatt, J. (1985). Fish Gill Structural Changes Induced by Toxicants and Other Irritants: A Statistical Review. *Canadian Journal of Fisheries and Aquatic Sciences*, 42, 630-648.

Marchant, R., & Banat, I. (2012). Microbial biosurfactants: Challenges and opportunities for future exploitation. *Trends in Biotechnology*, 30(11), 558-565.

National Petroleum Council. (1984). *Enhanced Oil Recovery*. Washington D.C.: National Petroleum Council.

Nguyen, T. T., Edelen, A., Neighbors, B., & Sabatini, D. A. (2010). Biocompatible lecithin-based microemulsions with rhamnolipid and sophorolipid biosurfactants: Formulation and potential applications. *Journal of Colloid and Interface Science*, 348, 498-504.

Nouraei, M., & Acosta, E. J. (2017). Predicting solubilisation features of ternary phase diagrams of fully dilutable lecithin linker microemulsions. *Journal of Colloid and Interface Science*, 495, 178-190.

Ojukwu, C., Onyekonwu, M., Ogolo, N., & Ubani, C. (2013). Alkaline Surfactant Polymer (Local) Enhanced Oil Recovery: An Experimental Approach. *SPE International*. The Society of Petroleum Engineers.

Patel, R., & Desai, A. (1997). Biosurfactant Production by Pseudomonas Aeruginosa GS3 from Molasses. *Letters in Applied Microbiology*, 25, 91-94.

Pitterer, C., Sellers, J., Janzen, D., Koch, D., Rothgeb, T., & Hunnicutt, M. (1993). Environmental Life-Cycle Inventory of Detergent-Grade Surfactant Sourcing and Production. *Journal of the American Oil Chemists' Society*, 70, 1-15.

Poremba, K., Gunkel, W., Lang, S., & Wagner, F. (1991). Toxicity Testing of Synthetic and Biogenic Surfactants on Marine Microorganisms. *Environmental Toxicology and Water Quality*, 6, 157-163.

- Rebello, S., Asok, A. K., Mundayoor, S., & Jisha, M. (2014). Surfactants: toxicity, remediation and green surfactants. *Environmental Chemistry Letters*, 12, 275-287. doi:10.1007/s10311-014-0466-2
- Riehm, D. A., Neilsen, J. E., Bothun, G. D., John, V. T., Raghavan, S. R., & McCormick, A. V. (2015). Efficient dispersion of crude oil by blends of food-grade surfactants: Toward greener oil-spill treatments. *Marine Pollution Bulletin*, 101, 92-97.
- Rocchio, J., Neilsen, J., Everett, K., & Bothun, G. D. (2017). A solvent-free lecithin-Tween 80 system for oil dispersion. *Colloids and Surfaces A*, 533, 218-233.
- Rocha, C., San-Blas, F., San-Blas, G., & Vierma, L. (1992). Biosurfactant production by two isolates of *Pseudomonas aeruginosa*. *World Journal of Microbiology and Biotechnology*, 8, 125-128.
- Roehl, P., & Choquette, P. (1985). *Carbonate Petroleum Reservoirs*. New York: Springer.
- Romanelli, M., Moraes, M., Villavicencio, A., & Borrely, S. (2004). Evaluation of Toxicity Reduction of Sodium Dodecyl Sulfate Submitted to Electron Beam Radiation. *Radiation Physics and Chemistry*, 71, 411-413.
- Rosen, M. J., & Kunjappu, J. T. (2012). *Surfactants and Interfacial Phenomena* (4th ed.). Hoboken, New Jersey, United States of America: John Wiley & Sons.
- Salager, J. (1999). Microemulsions. In G. Broze, *Handbook of Detergents - Part A: Properties* (pp. 253-302). New York: Marcel Dekker Inc.
- Salager, J., Forgiarini, A., & Bullon, J. (2013). How to attain an ultralow interfacial tension and a three-phase behavior with a surfactant formulation for enhanced oil

- recovery: a review. Part 1. Optimum formulation for simple surfactant–oil–water ternary systems. *Journal of Surfactants and Detergents*, 14(4), 449-472.
- Salager, J., Morgan, J., Schechter, R., Wade, W., & Vasquez, E. (1979). Optimum formulation of surfactant/water/oil systems for minimum interfacial tension or phase behavior. *Society of Petroleum Engineers Journal*, 107-115.
- Santa, M., Alvarez-Jurgenson, G., Busch, S., Birnbrich, P., Spindler, C., & Brodt, G. (2011). Sustainable Surfactants in Enhanced Oil Recovery. *Society of Petroleum Engineers*. Kuala Lumpur: SPE International.
- Shafeeq, M., Kokub, D., Khalid, Z., Khan, A., & Malik, K. A. (1989). Degradation of different hydrocarbons and production of biosurfactant by *Pseudomonas aeruginosa* isolated from coastal waters. *MIRCEN Journal*, 5, 505-510.
- Sheng, J. (2011). *Modern Chemical Enhanced Oil Recovery*. Amsterdam; Boston: Gulf Professional Publishing.
- Shinoda, K., & Arai, H. (1964, February 5). The Correlation Between Phase Inversion Temperature in Emulsion and Cloud Point in Solution of Nonionic Emulsifier. *The Journal of Physical Chemistry*, 3485-3490.
- Stalmans, M., Berenbold, H., Berna, J., Cavalli, L., Dillarstone, A., Franke, M., . . . Rappert, T. (1995). European Life-Cycle Inventory for Detergent Surfactants Production. *Tenside Surfactants Detergents*, 32(2), 84-109.
- Susmi, T., Rebello, S., Jisha, M., & Sherief, P. (2010). Toxic Effects of Sodium Dodecyl Sulfate on Grass Carp *Ctenopharyngodon idella*. *Fishing Technology*, 47(2), 157-162.

- Torres, L., Moctezuma, A., Avendano, J. R., Munoz, A., & Gracida, J. (2011). Comparison of bio- and synthetic surfactants for EOR. *Journal of Petroleum Science and Engineering*, 76, 6-11.
- van Nieuwenhuyzen, W. (2010). Lecithin and Other Phospholipids. In M. Kjellin, & I. Johansson, *Surfactants from Renewable Resources* (pp. 191-212). West Sussex, United Kingdom: John Wiley & Sons.
- Williams, H. D., Zlosnik, J. E., & Ryall, B. (2007). Oxygen, Cyanide and Energy Generation in the Cystic Fibrosis Pathogen *Pseudomonas aeruginosa*. *Advances in Microbial Physiology*, 52, 1-71. doi:10.1016/S0065-2911(06)52001-6
- Winsor, P. (1954). *Solvent Properties of Amphiphilic Compounds*. London: Butterworth's Scientific Publications.
- Xiangdong, F., Qinhong, W., Baojun, B., Xi Cai, L., Yongchun, T., Shuler, P. J., & Goddard, W. A. (2007). Engineering Bacteria for Production of Rhamnolipid as an Agent for Enhanced Oil Recovery. *SPE International*. Houston, Texas: Society of Petroleum Engineers.
- Yin, D.-Y., & Zhang, X.-R. (2013). Evaluation and research on performance of a blend surfactant system of alkyl polyglycoside in carbonate reservoir. *Journal of Petroleum Science and Engineering*, 111, 153-158.
- Zajic, J., Guignard, H., & Gerson, D. (1977). Properties and Biodegradation of a Bioemulsifier from *Corynebacterium Hydrocarboclastus*. *Biotechnology and Bioengineering*, 19, 1303-1320.

# VITAE

Name: Ahmed Saeed Al-Ghamdi

Nationality: Saudi Arabian

Date of Birth: April 5<sup>th</sup>, 1989

Email Address: ghamas1989@gmail.com

Address: P.O. Box 1140

Dhahran, 31311

Eastern Region

Kingdom of Saudi Arabia

Academic Background: Bachelor of Science in Computer Science (2011)